EFFECTS OF OPTICAL NONLINEARITIES ON FREQUENCY MULTIPLEXED SINGLE MODE OPTICAL FIBER SYSTEMS

by

JEROME D. ABERNATHY
B.S., Howard University (1981)
S.M., Massachusetts Institute of Technology (1984)

SUBMITTED IN PARTIAL FULFILLMENT OF THE
REQUIREMENTS FOR THE DEGREE OF

DOCTOR OF PHILOSOPHY
IN ELECTRICAL ENGINEERING AND COMPUTER SCIENCE

at the

MASSACHUSETTS INSTITUTE OF TECHNOLOGY
May 1987

Signature of Author_____
Department of Electrical Engineering and Computer Science

Certified by _____
Robert S. Kennedy
Thesis Supervisor

Accepted by _____
Arthur C. Smith
Chairman, Departmental Committee on Graduate Students

EFFECTS OF OPTICAL NONLINEARITIES ON FREQUENCY MULTIPLEXED SINGLE MODE OPTICAL FIBER SYSTEMS

by

JEROME D. ABERNATHY

Submitted to the Department of Electrical Engineering and Computer Science on May 1, 1987, in partial fulfillment of the requirements for the Degree of Doctor of Philosophy in Electrical Engineering and Computer Science

ABSTRACT

In order to fully exploit the capacity of single mode optical fibers, frequency multiplexing is currently being explored as a transmission scheme. If frequency multiplexing is used with a large number of channels, there arises the possibility that nonlinearities within the fiber may cause unacceptable interchannel interference or crosstalk. The purpose of this disseration is to explore the effects of two of these nonlinearities, stimulated four wave mixing and stimulated Raman scattering, from a communication system perspective. This is accomplished by modeling stimulated four wave mixing and stimulated Raman scattering as noises that are dependent on the system characteristics. We then find the structure and performance of optimal and suboptimal receivers for signals corrupted by these nonlinear noises.

Supervisor: Robert S. Kennedy

Professor of Electrical Engineering and Computer Science

TABLE OF CONTENTS

I Introduction

1.1 Motivation

Because of their huge capacity, single mode optical fibers have grown in popularity as communication media. Large volumes of information that once required bulky cables can be transmitted over a single hair-like fiber. Yet, because of speed limitations of the interface electronics and other considerations, the capacity of single mode fibers cannot now be fully exploited using time division schemes. Consequently, researchers are investigating the use of frequency division multiplexing as a transmission scheme. With frequency multiplexing, the transmission capacity is limited by the ability to generate and filter signals of different carrier frequencies rather than by the speed of the interface electronics.

If frequency multiplexing with a large number of channels is used, there arises the possibility that nonlinearities in the fiber may cause unacceptable interchannel interference or crosstalk [Stolen 80, 82]. Indeed, researchers have experimentally determined that, under certain conditions, nonlinearities may be the limiting factor in optical fiber communication systems [Tomita 83,Waarts 86].

The nonlinear effects of primary interest are stimulated Raman scattering (SRS) and stimulated four wave mixing. Fig. 1 gives a qualitative feel for these effects. Raman scattering [Smith 72, Chraplyvy 83] transfers power from high frequency signals to the

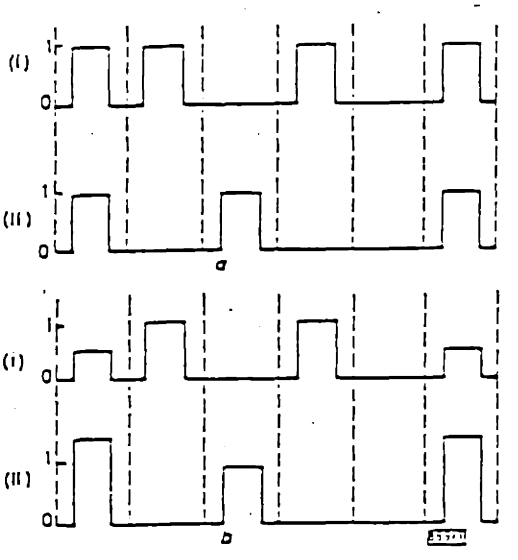

a Bit pattern in channels 1 and 2 with no stimulated Raman interaction
b Bit pattern in channels 1 and 2 with stimulated Raman interaction
(I) Channel 1
(II) Channel 2
When there is a mark simultaneously in both channels, the bit in channel 1 is depleted whereas the bit in channel 2 is amplified

Figure 1A

Stimulated Raman Scattering

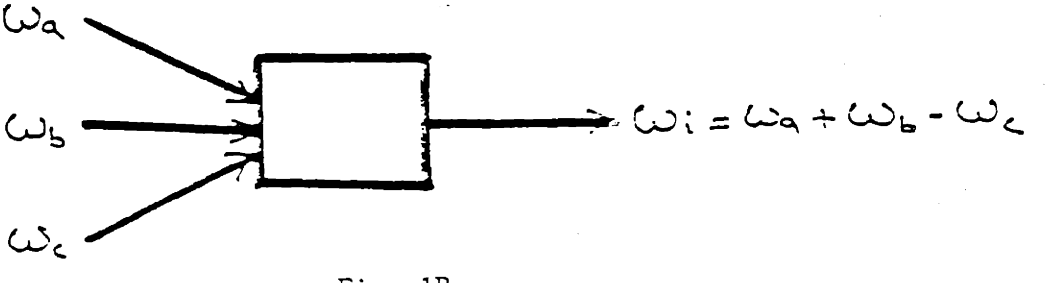

Fig. 1B

Stimulated Four Wave Mixing

lower frequency signals. From Fig. 1A we see that this occurs only when power is present at the same instant in both channels. The rate at which power is transferred is dependent on the average signal intensities and the frequency spacing between the channels. In multichannel systems, each channel will experience different levels of amplification and depletion. The lowest frequency channel is amplified while the highest frequency channel experiences pure depletion. The channels in between these two extremes experience either amplification or depletion depending on the number of channels above and below the channel carrier frequency. The highest frequency channel is the worst case channel because it is subjected to the most depletion.

Stimulated four wave mixing [Stolen 82, Hill 78] is depicted in Fig. 1B. Four wave mixing occurs when signals at three frequencies combine to produce signals at other frequencies. For multichannel systems, the interference in any particular channel due to four wave mixing is the sum of all the mixing terms that fall into the frequency of interest. The amplitude of any particular mixing term is dependent on the signal powers, the length of fiber, and the fiber dispersion characteristics. For frequency multiplexed systems with many closely spaced active channels, we expect to see significant levels of crosstalk.

If frequency multiplexing is to be used on a large scale within optical fiber networks, it is important to understand the limitations imposed by the nonlinearities on the system design. The

focus of this dissertation is to examine the effects of these nonlinearities on frequency multiplexed communication systems employing single mode optical fiber from a communication systems perspective.

1.2 Previous Research on Nonlinearities in Fiber

The nonlinear properties of optical fibers have been studied extensively [Stolen 79]. Most of the work has centered on analyzing the physics of the phenomena rather than their effects on communication system performance. Stimulated four wave mixing, stimulated Raman scattering, and self phase modulation are the nonlinear effects that have received the most attention. Four wave mixing in fibers has been studied mainly for parametric amplification applications [Stolen 82]. Stimulated Raman scattering has also been studied for amplification as well as frequency translation [Pochelle]. Some experiments have been performed to ascertain the effects of nonlinearities on the performance of specific communication systems. However, these studies concentrated on physical performance metrics such as levels of depletion rather than communication systems oriented measures such as bit error rate.

Stimulated Raman Scattering

Several experiments concerning the effects of stimulated Raman scattering on wavelength division multiplexed (WDM) systems have been published (WDM is distinguished from frequency multiplexing by it's wider channel spacing). Tomita [Tomita 83] performed experiments to determine the levels of crosstalk induced by

stimulated Raman scattering in two channel WDM systems. Using 1.0mw. intensity modulated signals at 1.26um. and 1.34um., Tomita measured crosstalk of -25dB. (in optical power) in 25km. of single mode fiber.

Chraplyvy and Henry [Henry 83] constructed a simulation to measure amplification of the long wavelength channel in a two channel system; the purpose being to investigate the use of Raman scattering for optical amplification. Chraplyvy also analytically approximated the worst case depletion of the shortest wavelength channel in a multichannel WDM system. He concluded that, for a ten channel system with 100nm. channel spacing, input powers should be at most 3.0mw. for depletion no worse than 0.5dB.

Stimulated Four Wave Mixing

The physics of four wave mixing in fibers has been extensively studied. Most of this research has focused on parametric amplification and techniques for phase matching to maximize gain [Stolen 75]. Recently, some analysis and experimentation has been done in the context of frequency multiplexed communication systems.

Hill, Kawasaki, Johnson, and McDonald investigated stimulated four wave mixing in single mode optical fibers [Hill 78]. They presented an analysis of phase matched four wave mixing and experimentally verified their results. Stolen has, over the years, published many papers on four wave mixing and phase matching techniques; most of this work is summarized in [Stolen 82]. The

fundamental conclusion from these papers is that four wave mixing in fibers is very sensitive to phase matching of the signals that are being mixed; we show later that this implies that four wave mixing is only a factor in frequency multiplexed systems that use low dispersion fiber or when the channels are closely spaced.

Waarts, Braun, and Shibata [Shibata 86, Waarts 86] simulated the effects of four wave mixing on a frequency multiplexed system possessing many channels. They determined the maximum average input power per channel allowable in order to limit the crosstalk induced into any channel for many combinations of fiber dispersion, attenuation, and fiber length.

1.3 Summary of Results

The purpose of the research contained in this dissertation was to determine the effects of stimulated Raman scattering and stimulated four wave mixing on frequency multiplexed communication systems employing single mode optical fiber. We determined the effects of these nonlinearities from a communication systems perspective by first modeling four wave mixing and Raman scattering as noise and then determining the structure and performance of the receivers used to detect signals corrupted by these nonlinear noises. Because each nonlinear effect dominates under unique conditions, we were able to consider four wave mixing and Raman scattering separately rather than attempting to analyze their combined effect.

The system model used for the analysis consisted of a point to point fiber link where N on-off modulated signals at sequentially spaced carrier frequencies are input into the fiber (Fig. 2). A quantum-limited heterodyne receiver at the end of the fiber is used for detection. For each nonlinear effect, any particular frequency channel could be modeled as a simple channel (Fig. 3) where a signal is corrupted by the nonlinear interference and shot noise from the local oscillator. Using this channel model and a description of the interference due to each nonlinearity, we then determined performance for a variety of receiver structures.

Stimulated Four Wave Mixing

We analytically determined the effects of stimulated four wave mixing on the performance of two system models. The first, the synchronous model, assumed the frequency channels were slotted in time so that pulses in different frequency channels in the same time slot would be synchronized. Also, the synchronous model assumed rectangular pulse shapes. As such, this represented a worst case scenario whose performance could be used as a lower bound for frequency multiplexed systems corrupted by four wave mixing. The second model, the general case, was much more realistic because assumptions about pulse shapes and synchronization were relaxed.

We determined that, for the general case, the interference amplitude caused by stimulated four wave mixing could be modeled as

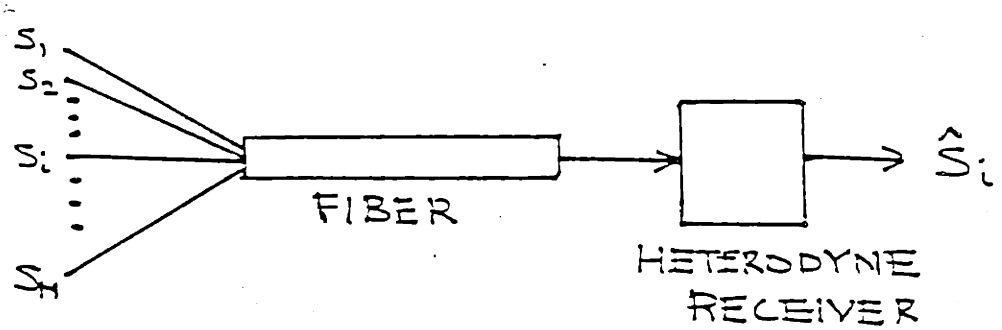

Figure 2

System Model

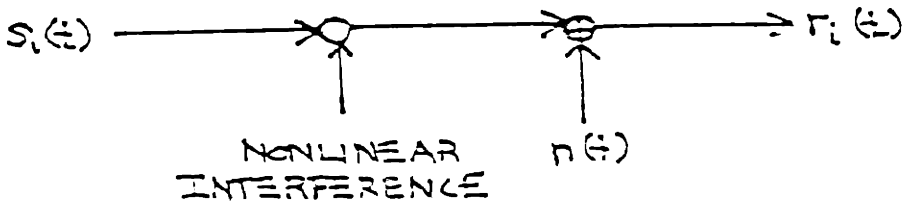

Figure 3

Channel Model

an additive zero-mean Gaussian noise with correlation function

$$R_I(\tau) = 2\sigma_I^2/T^3 \; [p(\tau)*p(\tau)]^3$$

where p(t) is a symmetric amplitude pulse shape (* denotes convolution), T is the spacing between pulses, and σ_I^2 is a parameter dependent on the fiber dispersion characteristics and other system parameters such as number of channels, signal powers, length of the fiber, etc. In order to experience significant levels of interference, the differences in phase velocity ("phase matching") between the channels had to be very small. This occured when either the fiber dispersion was very low- such as with dispersion shifted or dispersion flattened fiber- or the channels were spaced very closely together. σ_I^2 for a phase matched system is described by

$$\sigma_I^2 = M_N(i)B^2P^3(\; 1 - e^{-2\alpha L} \;)^2$$

where $M_N(i)$ is the number of mixing permutations that fall into channel i, α is the fiber attenuation constant, B is dependent on the fiber attenuation, L is the fiber length, and P is the probability that a pulse is "on". For phase matched systems, the interference induced into any particular channel is determined to a large extent by $M_N(i)$. $M_N(i)$ is plotted in Fig. 4 for a 10,000 channel system.

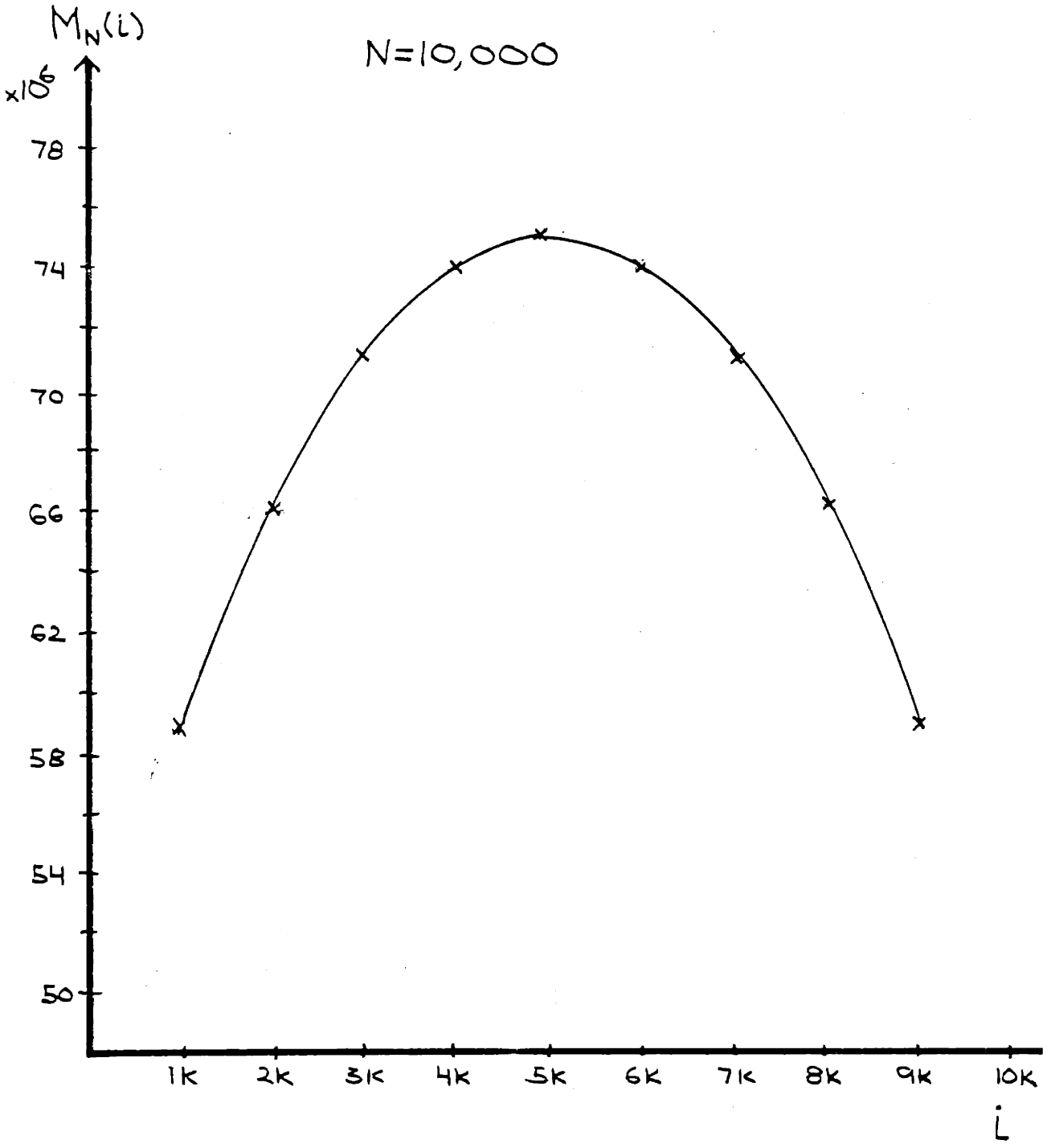

Figure 4

$M_N(i)$ vs. i for $N = 10^4$

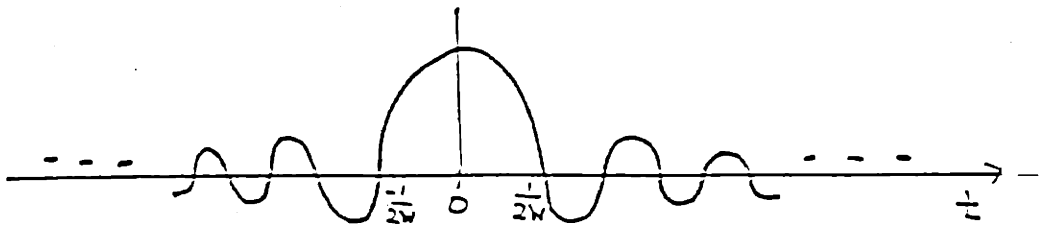

Figure 5

Sinc Pulse

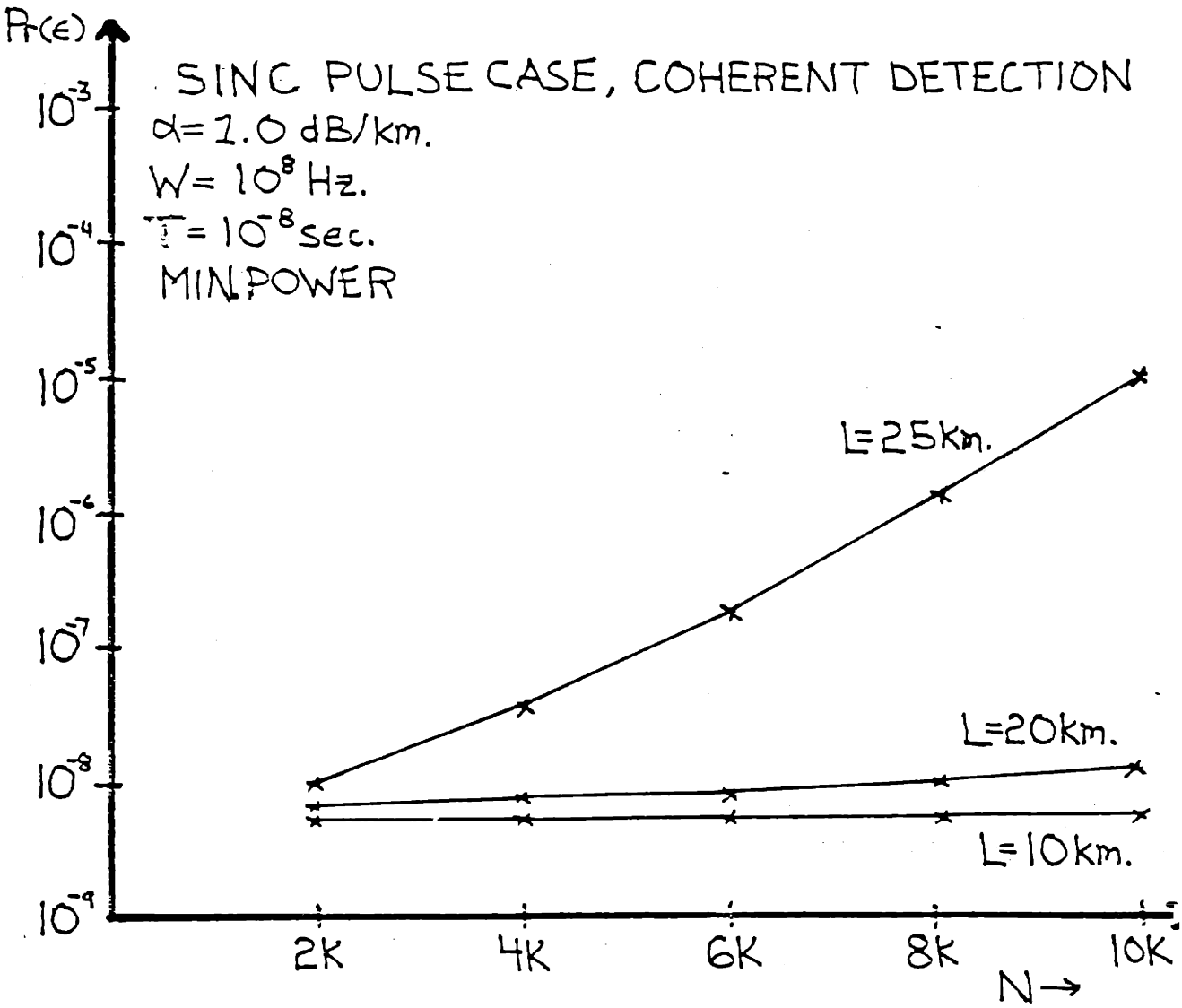

Figure 6

Pr(ϵ) vs. N for Stimulated Four Wave Mixing

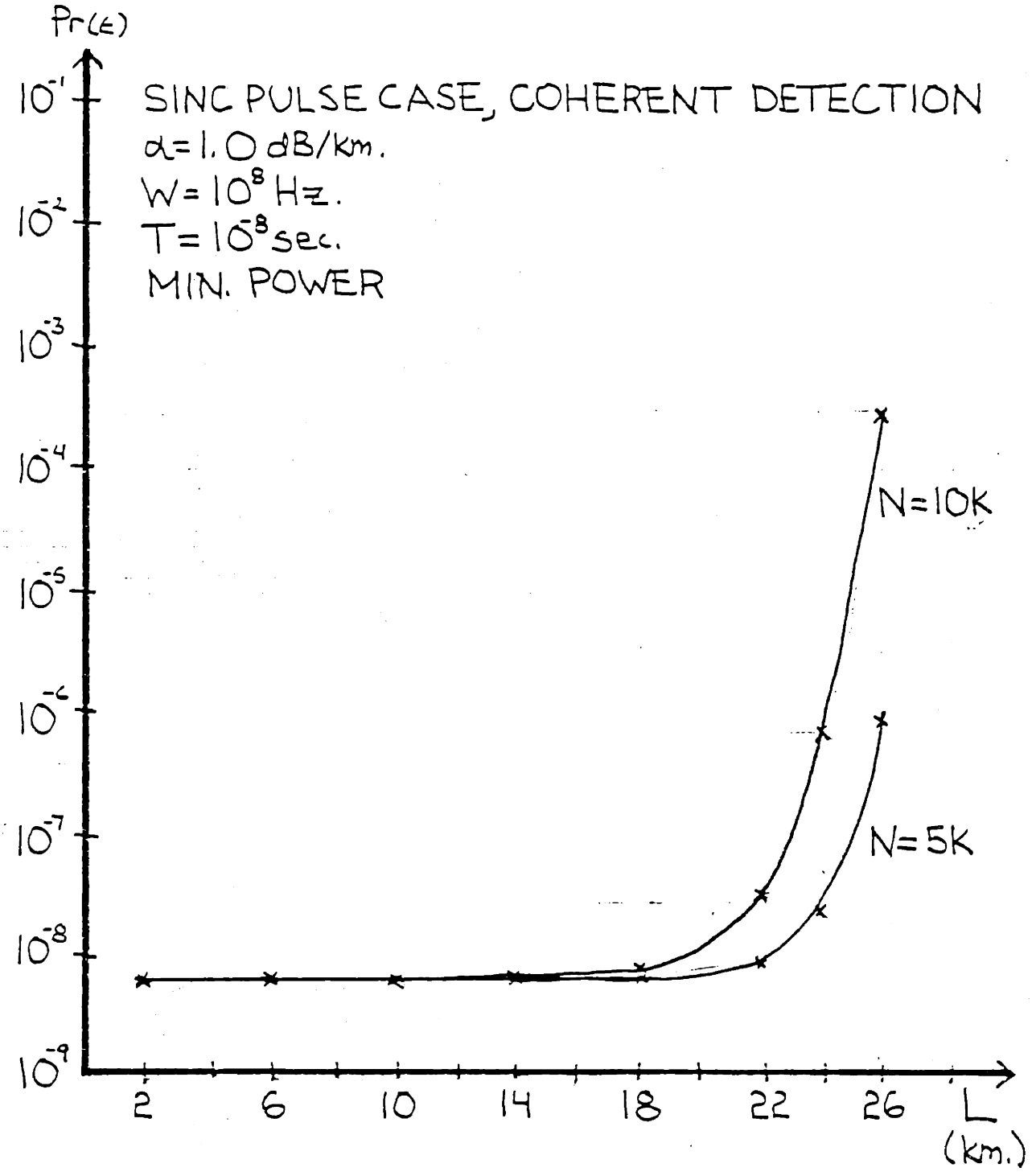

Figure 7

Pr(ε) vs. L for Stimulated Four Wave Mixing

Using the above description of the four wave mixing interference, we determined the performance of a variety of receiver structures assuming that p(t) was a sinc pulse (Fig. 5) and that the systems were phase matched. The receiver structures were:

* Optimal coherent detector
* Optimal incoherent detector
* Suboptimal coherent matched-filter detector.

Comparing the performance of these receivers, we found that the incoherent and matched filter receivers performed virtually the same as the optimal coherent detector.

From the performance analysis results we determined the effects of stimulated four wave mixing interference on this particular system when the number of channels is large. We found that the degradation in system performance is only a factor when the fiber is long (L > 25km.) and the number of channels is large. For shorter fiber lengths the stimulated four wave mixing interference is negligible irrespective of the number of channels. This is illustrated in Fig. 6 and Fig. 7 where we have plotted the probability of error in the worse case channel for numbers of channels and fiber lengths. For each length of fiber we set the average input power per channel to yield a 10^{-9} bit error rate in the absence of four wave mixing interference (approximately 10^{-8} Watts for L=25km.). The worst case channel, i=N/2, provides a good estimate of the performance in most of the channels because of the gradual roll-off of $M_N(i)$.

Stimulated Raman Scattering

Using the synchronous system model, we determined that, for systems with large numbers of channels, stimulated Raman scattering in the highest frequency channel (which is the worst case channel) could be modeled as log-normal fading. This is depicted in Fig. 8 where the Raman fading is a multiplicative channel noise where the noise is log-normal distributed. The signals in any particular time slot were modeled as

$$E(\omega_i, L) = Ee^{-\alpha L} X_i$$

where the exponential term accounts for fiber attenuation and the X_i is a modulation random variable that is one with probability P and zero with probability 1-P. Given these signals, the received signal in the worst case channel is of the form

$$r(\omega_N, L) = EX_N G(L) e^{-\alpha L} + n(t)$$

$$G(L) = e^{-x}$$

where n(t) is the white noise and G(L) is the Raman fade random variable. x is a Gaussian random variable whose mean and variance are dependent on the the system and fiber parameters:

$$E(x) = (L_{eff} P(0) / A_{eff}) P \sum_j \tau_j$$

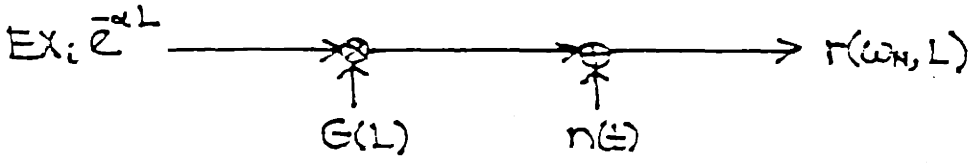

Figure 8

Stimulated Raman Scattering Channel Model

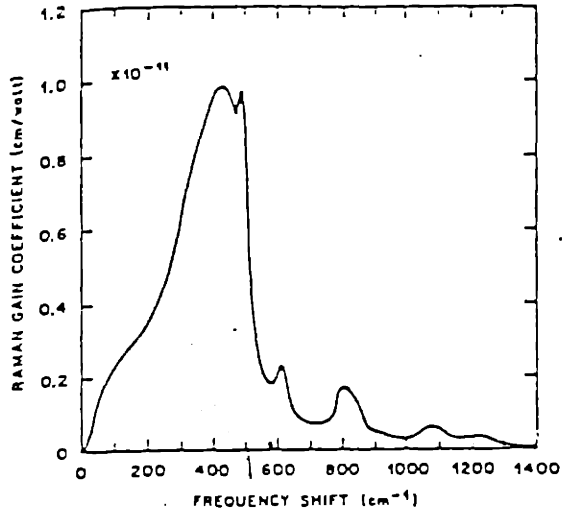

Figure 9

Raman Gain Coefficient vs. Channel Frequency Seperation

$$\sigma_x^2 = (L_{eff}P(0)/A_{eff})^2(P-P^2)\sum_j \gamma_j^2$$

where $$L_{eff} = (1-e^{-\alpha L})/\alpha$$

and j is summed between 1 and N-1. A_{eff} is the effective cross sectional area of the fiber, P(0) is the bit input power, P is the probability that a pulse is on, and γ_j is the Raman gain coefficient that couples channel j with the worst case channel. The Raman gain coefficient versus frequency separation is shown in Fig. 9.

Determining the performance of the optimal receiver for this system was analytically intractable. So rather than using the optimal receiver for our system, we resorted to a receiver structure that assumed knowledge of the fade random variable. The detection problem can be viewed as in Fig. 10 where a fade causes the two white noise densities to move closer together- thereby increasing the probability of error due to the additive white noise. The receiver we used would set the optimal threshold given the fade parameter. Thus, for any particular value of G(L), this receiver would pick a threshold that was halfway between the means of the two a posteriori densities. Clearly, this performs better than the optimal fixed threshold receiver. When the standard deviations of the noise densities are small compared to the bit energy, this receiver gives reasonable, albeit optimistic, results because the fade must be very deep in order to see any significant change in $Pr(\epsilon)$ (Fig. 11). The performance for this receiver was measured in terms of the

Figure 10

Raman Fading

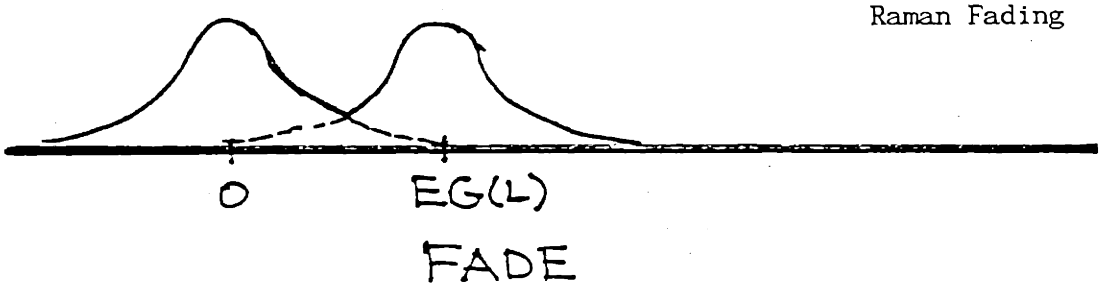

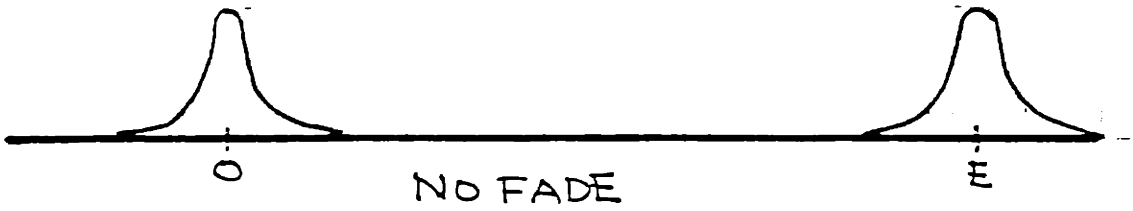

Figure 11

Raman Fading for High SNR System

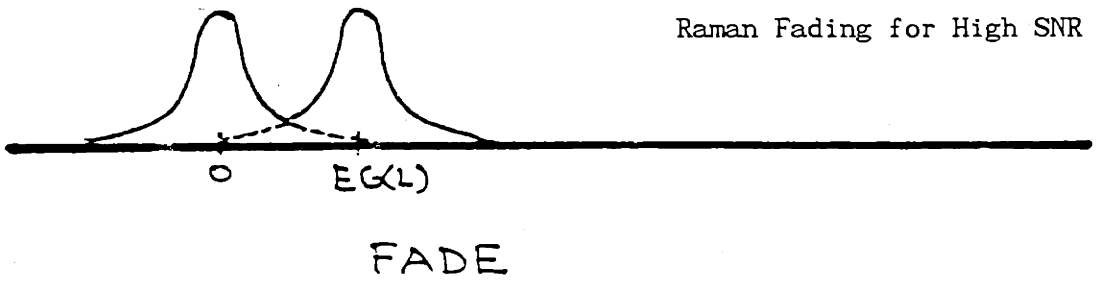

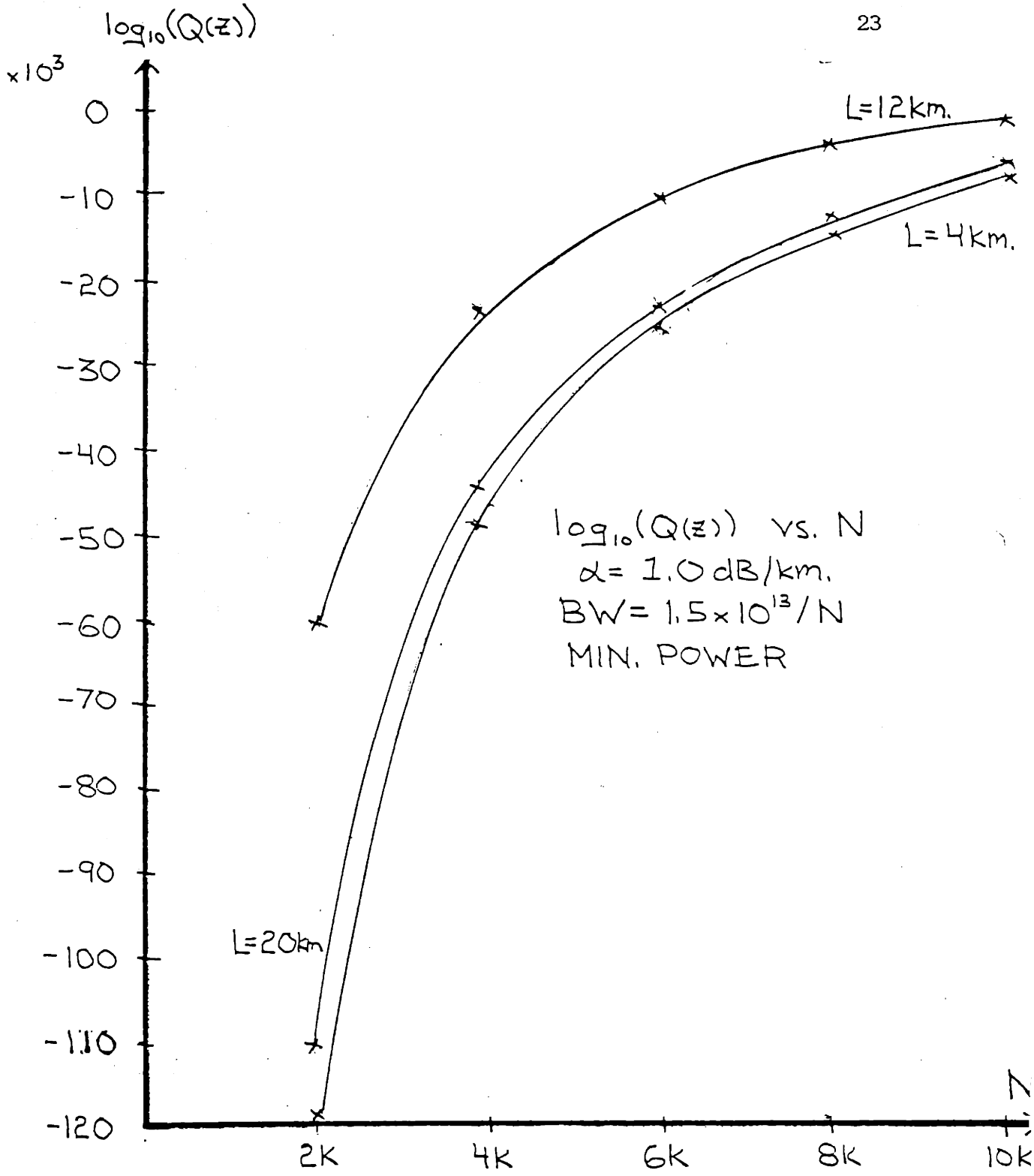

Figure 12

Performance in Presence of Raman Fading, Minimum Power

percentage of time that the fade was deep enough to cause $Pr(\epsilon)$ to exceed some threshold. Given that the link power budget for each fiber length was set to yield a 10^{-9} bit error rate in the absence of Raman scattering, we set our threshold to 10^{-6}. For each N the channels were evenly spaced so they would occupy the entire Raman gain band (0 to 450 cm^{-1}).

Using these results we were able to determine under what scenarios Raman fading is a factor. Setting

$$\% \text{ time } Pr(\epsilon) \geq 10^{-6} = Q(Z)$$

(where Q(Z) is Marcum's Q function and Z is dependent on the system parameters) we plotted $\log_{10}(Q(Z))$ versus the number of channels for various fiber lengths in Fig. 12. We see from Fig. 12 that the chances of seeing a deep fade are practically nil. Thus, we concluded that, even for moderately long (25km.) fiber lengths and large numbers of channels, stimulated Raman scattering was not an important factor. The primary reason for this result is that, for systems that have large numbers of channels, the signal input powers are too low to stimulate significant Raman interaction.

1.4 Overview of Thesis

In chapter II we will introduce the physics of nonlinearities in fiber and the modeling assumptions that will be used throughout the analysis.

Chapter III examines the effects of four wave mixing on frequency multiplexed digital communication systems employing single mode fiber. We will start by analyzing the synchronous system model to establish performance lower bounds and gain familiarity with the analysis. We will then analyze a much more realistic digital communication system model. Finally, the results of the analysis will be examined to determine under what scenarios four wave mixing degrades system performance.

Chapter IV analyzes the effects of stimulated Raman scattering on frequency multiplexed digital communication systems. The synchronous system model is analyzed in the presence of Raman scattering. The optimal receivers are discussed and bounds are derived for the performance of an idealized receiver. The results are then examined to determine the effects of stimulated Raman scattering on foreseeable communication systems.

This thesis examines the effects of nonlinearities on point to point links that utilize frequency multiplexing. However, frequency multiplexing is also being considered for use in fiber networks. Therefore, we wrap up the thesis by suggesting issues for the examination of nonlinear effects in optical fiber networks that utilize frequency multiplexing and single mode optical fiber.

II The Physics of Nonlinearities in Fiber

2.1 Basic Theory

In this section we review the physics of stimulated four wave mixing and stimulated Raman scattering scattering in fiber. The purpose of this review is to develop the theory needed to analyze the effects of nonlinearities on frequency division multiplexed systems using single mode optical fiber. We will begin our discussion with a general description of waves in nonlinear media which will then be extended to fiber and our specific applications.

The nonlinear interaction of waves in a medium can be described by a set of coupled wave equations where the nonlinear susceptabilities act as coupling coefficents. Stimulated four wave mixing and stimulated Raman scattering are distinguished by the form of the coupling but they are special cases of the same nonlinear phenomenon.

For a general description of the propagation of plane waves in nonlinear media, we start with Maxwell's equations

$$\nabla \times \bar{E} = - \frac{d\bar{B}}{dt}$$

$$\nabla \times \bar{H} = \frac{d\bar{D}}{dt} + \bar{J}$$

and the constitutive relations

$$\bar{B} = \mu_o \bar{H}$$

$$\bar{D} = \epsilon_o \bar{E} + \bar{P}$$

$$\bar{J} = \sigma \bar{E}.$$

Using the above equations and forming a wave equation

$$\nabla \times \nabla \times \bar{E} = \nabla(\nabla \cdot \bar{E}) - \nabla^2 \bar{E} = -\mu_o \frac{d}{dt} (\nabla \times \bar{H})$$

and assuming that $\nabla \cdot \bar{E} = 0$ we conclude that

$$\nabla^2 \bar{E} - \mu_o \sigma \frac{d\bar{E}}{dt} - \mu_o \epsilon_o \frac{d^2 \bar{E}}{dt^2} = \mu_o \frac{d^2 \bar{P}}{dt^2}.$$

By expanding the polarization, P, into linear and nonlinear parts the above equation becomes [Ippen 85]

$$\nabla^2 \bar{E} - \mu_o \sigma \frac{d\bar{E}}{dt} - \mu_o \epsilon_o \frac{d^2}{dt^2} \{ (1 + \chi^{(1)}) \bar{E} \} = \mu_o \frac{d^2 \bar{P}_{NL}}{dt^2}$$

where $\chi^{(1)}$ is the first order susceptability term. This wave equation describes the interaction of an E field and the nonlinear polarization term in a nonlinear medium. The polarization can be considered to be the driving term of a system. As such, P_{NL} can, depending on the phase difference between P_{NL} and E, add or remove power from the E field.

For monochromatic TEM waves propagating in the z direction, we can approximate the E field and P_{NL} as slowly varying envelopes times an oscillatory term

$$\bar{E}(\omega,z,t) = \hat{e}\, E(z,t)\, e^{-j(kz - \omega t)}$$

$$\bar{P}_{NL}(\omega,z,t) = \hat{p}\, P_{NL}(z,t)\, e^{-j(k_p z - \omega t)}.$$

Plugging these expressions into our wave equation and assuming the waves do not change appreciably over a wavelength or one period we find

$$\frac{dE}{dz} + \alpha E + (n/c)\frac{dE}{dt} = -\frac{j\omega\mu_o c}{2n}(\hat{e}\cdot\hat{p})\, P_{NL}\, e^{j(k - k_p)z}$$

where we have assumed the waves are one-dimensional and that

$$\omega^2 P_{NL} >> \omega\frac{dP_{NL}}{dt} >> \frac{d^2P_{NL}}{dt^2}.$$

α is the material attenuation constant, n is the refractive index, and c is the speed of light. Notice the solution to the above differential equation is dependent on the relative phase of E and P_{NL}. By properly choosing P_{NL}, the resulting E field can, as a function of z, monotonically grow, oscillate, or montonically decrease in intensity.

For our purposes we will assume that the waves vary slowly enough as they traverse the medium to allow a quasi-static approximation to the above equation

$$\frac{dE}{dz} + \alpha E = - \frac{j\omega\mu_o c}{2n} (\hat{e} \cdot \hat{p}) P_{NL} e^{j(k - k_p)z}$$

where we have set $\frac{dE}{dt} = 0$.

Expanding P_{NL} we see

$$P_{NL} = \epsilon_o(\chi^{(2)}E^2 + \chi^{(3)}E^3 + \chi^{(4)}E^4 + \ldots)$$

where $\chi^{(i)}$ is the i^{th} order nonlinear susceptability term (we assume $\{\chi^{(i)}\}$ are independent of frequency). Glass (the material of which optical fiber is made) possesses a property known as inversion symmetry according to which every even order nonlinear susceptability term is zero. Therefore, for our purposes,

$$P_{NL} = \epsilon_o(\chi^{(3)}E^3 + \chi^{(5)}E^5 + \ldots).$$

The third order susceptability term, $\chi^{(3)}$, is responsible for stimulated four wave mixing and stimulated Raman scattering. $\chi^{(3)}$ is complex with the real part leading to four wave mixing and the imaginary part giving stimulated Raman scattering in fiber. For the study of four wave mixing and Raman scattering we can can truncate

the series expansion of P_{NL} to yield

$$P_{NL} = \epsilon_o \chi^{(3)} E^3.$$

2.2 Stimulated Four Wave Mixing in Fiber

Stimulated four wave mixing is similar to third order intermodulation distortion in radio frequency systems; signals at three carrier frequencies mix to produce interference at a fourth carrier frequency. Stimulated four wave mixing is characterized by its nonlinear polarization term. For our analysis we are interested in the four wave mixing polarization term that occurs when N plane waves at frequencies $\{\omega_i\}$ and propagation constants $\{k_i\}$ propagate through a nonlinear medium. We are interested in mixing terms of the form $\omega_i = \omega_a+\omega_b-\omega_c$, $a,b \neq c$ because this is the only mixing combination of interest that results in frequencies that fall in the communication system channels. This polarization can be expressed as

$$P_{NL}(\omega_i,L,t) = 3\epsilon_o\chi^{(3)} \sum_a \sum_b \sum_c E(\omega_a,L,t)E(\omega_b,L,t)E^*(\omega_c,L,t)$$
$$\cdot\delta(i-(a+b-c))$$

where $\delta(\ )$ is a kronecker delta used to select the terms such that $i=a+b-c$ and a,b,c are summed from 1 to N except i and L is the length of the fiber. By plugging in the slowly varying envelope representations of the fields we find

$$P_{NL}(\omega_i,L)=3\epsilon_o\chi^{(3)}\sum_{a,b,c} E(\omega_a,L)E(\omega_b,L)E^*(\omega_c,L)e^{-j(k_a+k_b-k_c)L}\delta(i-(a+b-c))$$

Looking at our wave equation again, it is apparent that the solution for E_i will be dependent on the phase differences of each term in the P_{NL} sum and E_i which are defined by

$$\Delta k = k_a + k_b - k_c - k_i .$$

For any $\Delta k = 0$, we find that E_i will grow monotonically until all the power has been depleted from the weakest contributing wave of the term in P_{NL}. However, for $\Delta k \neq 0$ the terms of E_i will oscillate with z at a rate dependent on the value of Δk. Therefore, to see significant levels of interaction due to four wave mixing the propagation constants must be very well matched (i.e. the Δk terms must be very small). In bulk materials this can be accomplished by adjusting both the direction and magnitude of the propagation vectors. However in single mode optical fiber the direction of propagation is fixed. This means, in order for Δk to be very small, the frequencies of the waves must be very closely spaced or the fiber dispersion over the frequency band must be very low (such as with dispersion flattened or dispersion shifted fibers). Δk in single mode optical fiber for large channel spacing ($\geq$1.0Ghz.) is approximated by [Waarts 86]

$$\Delta k_{abc} = 2\pi C\lambda^2 (\Delta f_{eq})^2 / c$$

$$\Delta f_{eq} = |(f_a - f_c)(f_b - f_c)|^{1/2}$$

where C is the fiber chromatic dispersion coefficent and λ is the wavelength of the center of the frequency band. With long fiber lengths and very low dispersion over the frequency band, four wave mixing will probably cause significant levels of crosstalk among frequency channels.

2.3 Stimulated Raman Scattering

Stimulated Raman scattering is very similar to four wave mixing because it is also a third order mixing phenomenon. It differs, however, because it is a noncoherent effect, i.e. it does not depend on the relative phases of the mixing waves. This is because stimulated Raman scattering is third order mixing between the channel of interest, i, and one other channel, a. This corresponds to mixing of the form $\omega_i = \omega_i + \omega_a - \omega_a$. The corresponding nonlinear polarization is

$$P_{NL}(\omega_i,L)= 3\epsilon_o\chi_r^{(3)} \sum_a E(\omega_i,L)\,|E(\omega_a,L)|^2\, e^{-jk_iL}$$

where a is summed from 1 to N except i and $\chi_r^{(3)}$ is the third order susceptability for stimulated Raman scattering. Notice that the stimulated Raman scattering P_{NL} is dependent only on the initial value of E_i and the intensities of the other contributing waves. It is not dependent on the relative phases of the waves This means that the intensity of E_i will grow as the waves propagate down the fiber until all of the power in the other waves has been depleted. The

rate of transfer is dependent on the the intensities of the waves and the stimulated Raman scattering coefficient at their frequencies.

In fiber, stimulated Raman scattering acts to transfer power from higher frequency channels to lower frequency channels. The rate of transfer is dependent on the wave intensities and frequency separations. Ignoring the power gain of the lower frequency waves and using the quasi static approximation, the power depletion of the highest frequency wave can be described as (see Chap. IV)

$$P_N(t,L) = P(t,L=0)\ e^{-\alpha L}\ \exp\left[-(L_{eff}/\ \alpha A_{eff})P(t,L=0) \sum_j \gamma_j \right]$$

$$L_{eff} = (1- e^{-\alpha L})/\alpha$$

where γ_j is the Raman gain between the wave at ω_j and the highest frequency wave at ω_N, A_{eff} is the effective cross section area of the fiber, and P(t,L=0) is the input (instantaneous) power pulse shape in each channel. j is summmed over the lower frequency channels. The Raman gain is plotted vs. frequency separation in Fig. 13.

Notice that the Raman gain is very low for closely spaced waves; the effect of Raman scattering will be very weak for this situation. However, because of good phase matching resulting from the waves being very closely spaced, stimulated four wave mixing will be

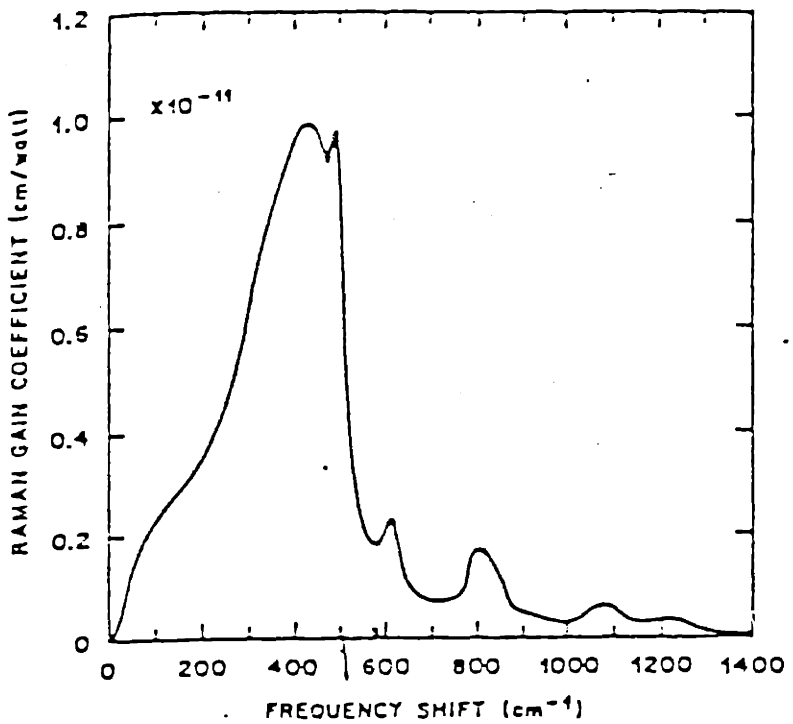

Figure 13

Raman Gain Coefficient vs. Channel Frequency Seperation

strong. Therefore, stimulated four wave mixing dominates when the waves are closely spaced in frequency (assuming nonzero fiber dispersion). Conversely, stimulated Raman scattering is strong for more widely spaced waves- therefore Raman scattering dominates when the waves are more widely spaced. For these two scenarios, we can examine each nonlinear effect in isolation.

III Effects of Stimulated Four Wave Mixing

3.1 Chapter Overview

In this chapter we will use the physics presented in Chap. II to determine the effects of four wave mixing on frequency division multiplexed systems employing single mode optical fiber. As we know, four wave mixing introduces crosstalk among the frequency channels. For any particular channel, this crosstalk can be considered to be an additive interference (Fig. 14) where the interference is dependent on the signals in the other channels, the length of the fiber, and other system parameters. Our task is to characterize this interference and then find the optimal receiver structure and it's corresponding performance.

We will examine two types of frequency division multiplexed systems. The first, the synchronized case, assumes bit synchronization among the frequency channels and rectangular pulse shapes. This will allow us to examine the system as if we were trying to detect continuous waves instead of modulated carriers. The synchronous model represents a worst case scenario that sets a lower bound on the performance of frequency multiplexed systems corrupted by the nonlinearities. The second case (which we shall refer to as the general case) is much more realistic in that it makes no assumptions about synchronization or the pulse shapes. Using this general model, we will determine the performance of a system that uses a particular pulse shape. Throughout our analysis we will assume on-off keying (OOK) modulation.

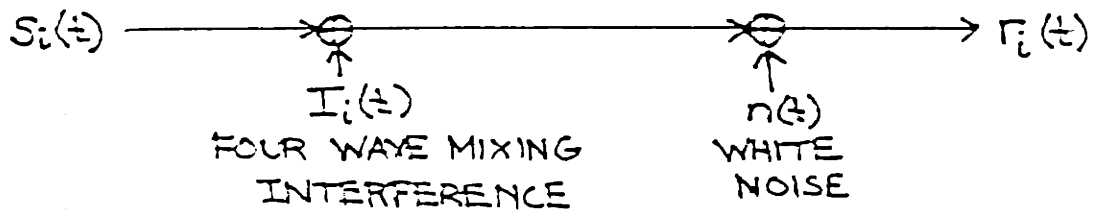

Figure 14

Stimulated Four Wave Mixing Channel Model

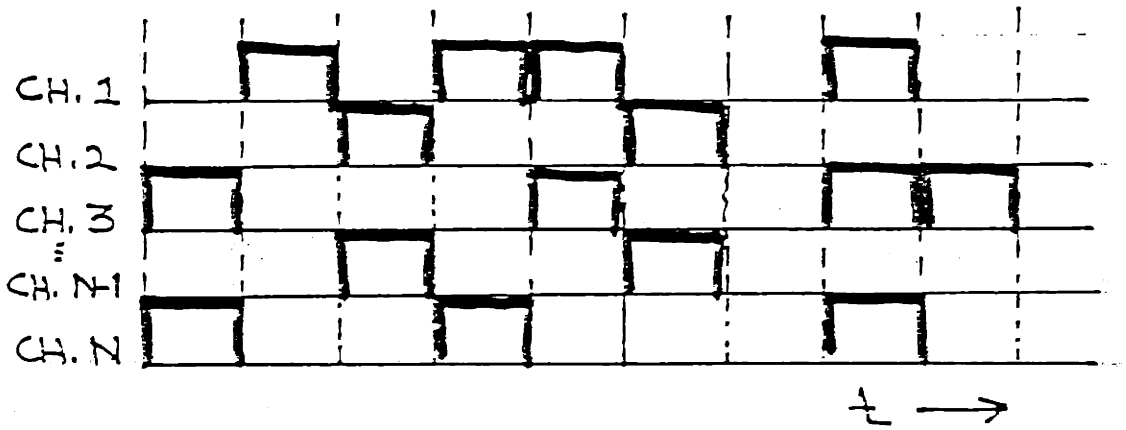

Figure 15

Synchronous System Model

3.2 The Synchronous Case

In this section we analyze the performance of frequency division multiplexed systems corrupted by four wave mixing interference assuming rectangular pulses and bit synchronization. Using a model of the system, we will characterize the four wave mixing interference as a random variable and determine it's statistics. We will then determine the structure of the optimal receiver and it's performance.

3.2.1 Communication System Model Description

The system we wish to analyze (Fig. 15) consists of N sequentially spaced frequency channels with carrier frequencies $\{\omega_i\}$ where

$$\omega_i = \omega_o + \Delta\omega i \; ; \; 1 \leq i \leq N.$$

The signals in each channel consists of OOK modulated carriers that are bit synchronized. In any particular bit slot these signals can be characterized by

$$\bar{E}(\omega_i, L, t) = \hat{e}\, E\, e^{-\alpha L} X_i \cos(\omega_i t + \phi_i - k_i L)$$

$$X_i = \begin{cases} 1 \; ; \; \text{w/ probability } P \\ 0 \; ; \; \text{w/ probability } 1-P \end{cases}$$

ϕ_i is phase R.V. uniform distributed $[-\pi, \pi]$

where X_i denotes the presence or absence of a pulse in channel i, ϕ_i is a phase random variable, L is the length of the fiber, and k_i is the propagation constant. We assume the waves are linearly polarized in the same direction. It is convenient to express the signals $\{E_i\}$ as

$$\bar{E}(\omega_i,L,t) = \hat{e}E(\omega_i,L)\, e^{j(\omega_i t - k_i L)}$$

$$E(\omega_i,L) = X_i E\, e^{j\phi_i}\, e^{-\alpha L}.$$

where α is the fiber attenuation constant. Throughout the analysis we will use the envelope of the signals ($E(\omega_i,L)$) without loss of generality. Using this model we see that the signal and four wave mixing interference envelopes will be constant over the duration of one bit. The four wave mixing interference simply adds a complex number to the pulse amplitude (which is also complex). The pulse is then further corrupted by additive white Gaussian noise caused by the shot noise from the local oscillator.

3.2.2 Characterization of Interference

Now that we have an idea of how the system looks, we must characterize the interference in any channel due to four wave mixing. We will define the interference amplitude in channel i as

$$I(\omega_i,L,t) = \hat{e}I(\omega_i,L)e^{j(\omega_i t - k_i L)}$$

$$I(\omega_i,L) = Ie^{-\alpha L}.$$

From chapter II we know the differential equation characterizing $I(\omega,L)$ can be expressed as

$$\frac{dI(\omega,L)}{dL} + \alpha I(\omega,L) = \frac{-j\omega\mu_o c}{2n} P_{NL}(\omega,L)e^{jkL}$$

$$\text{where } \bar{P}_{NL}(\omega,L,t) = \hat{e}P(\omega,L)e^{j\omega t}$$

where we have ignored the depletion of the signals that contribute to the mixing (ignoring the depletion of the signals is an appropriate assumption because the i^{th} channel will be swamped by the interference long before the depletion of any one channel becomes noticable).

Using the expression for $P_{NL}(\omega,L)$ given in chapter II and our signal model, we find

$$P_{NL}(\omega_i,L) = 3\chi^{(3)}\epsilon_o E^3 e^{-3\alpha L} \sum_a \sum_b \sum_c e^{j(\phi_a+\phi_b-\phi_c)} e^{-j(k_a+k_b-k_c)L} \cdot X_a X_b X_c \delta(i-(a+b-c))$$

where a,b,c are summed from 1 to N except i. We exclude the i^{th} term from the sum because we are interested in interference induced by other channels rather than terms that involve the signal itself (which actually contributes very little to the polarization term).

Substituting $I(\omega_i,L)e^{-jk_iL}$ and $P_{NL}(\omega_i,L)$ into the differential equation and solving we obtain

$$I(\omega_i,L)= B \sum_a \sum_b \sum_c \frac{e^{-j(\phi_a+\phi_b-\phi_c)}}{\Delta k_i - j2\alpha} \left[e^{-j(\Delta k_i - j2\alpha)L} - 1 \right]$$

$$\cdot e^{-\alpha L} X_a X_b X_c \delta(i-(a+b-c))$$

$$\text{where } B= \frac{\omega_i \mu_o c \epsilon_o 3E^3 \chi^{(3)}}{2n_i}$$

$$\text{and } \Delta k_i = k_a+k_b-k_c-k_i.$$

As expected, the terms in the sum representing $I(\omega_i,L)$ are dependent on the degree of phase matching which is determined by the difference in propagation constants, Δk_i. Each term in the sum oscillates with L with a period and amplitude determined by Δk_i. If Δk_i for a particular term is large, the amplitude of the term is small and oscillates very rapidly with L. On the other hand, if Δk_i is zero the term grows monotonically with L.

After deriving the function describing the complex envelope of the interference we must determine its statistics. Unfortunately, it appears quite difficult to determine the exact statistics of the interference. However, the complex envelope is the sum of a large number of complex mixing terms- many of which are mutually independent. It seems, therefore, appropriate to approximate the

interference envelope density as a complex Gaussian random variable. This will allow us to completely characterize the interference by it's first and second order moments.

Because $I(\omega_i,L)$ is a complex random variable, the jointly Gaussian random variable describing it is characterized by three expected values; $E(I(\omega_i,L))$, $E(I^2(\omega_i,L))$, and $E(|I(\omega_i,L)|^2)$. Remembering that $\{\phi_i\}$ are uniform distributed between $-\pi$ and π, it is easy to show that

$$E(I(\omega_i,L))= 0$$

$$E(I^2(\omega_i,L))= 0.$$

We also see that (Appendix A)

$$E(|I(\omega_i,L)|^2)= B^2P^3e^{-2\alpha L}\sum_a\sum_b\sum_c \frac{\delta(i-(a+b-c))}{\Delta k_i^2 + 4\alpha^2}$$

$$\cdot\left[\, 1+ e^{-4\alpha L} - 2e^{-2\alpha L}\cos\Delta k_i L \,\right].$$

If we assume perfect phase matching, i.e. $\Delta k_i \rightarrow 0$, we see that

$$E(|I(\omega_i,L)|^2)= (M_N(i)B^2P^3e^{-2\alpha L}/4\alpha^2)(1 + e^{-4\alpha L} - 2e^{-2\alpha L})$$

where $M_N(i)$ = # permutations such that $i=a+b-c$. $M_N(i)$ is given by (Appendix B):

$$M_N(i)= \begin{cases} N(N+2i-2) - (1/2)[(N+i)(N+i+1)+i(i+1)] + 3 \; ; \; 2\leq i\leq (N/2) \\ N(N+2i-4) - (1/2)[(N+i)(N+i+1)+i(i+1)] + (4i+1) \; ; \; N/2<i\leq N \end{cases}$$

Using these results we can find the covariance matrix for the joint density. We know that

$$I(\omega_i,L)= Re[I(\omega_i,L)] + jIm[I(\omega_i,L)].$$

We define the covariance matrix as

$$\bar{R}_I(\omega_i,L)= \begin{bmatrix} E(Re(I)^2) & E(Re(I)Im(I)) \\ E(Re(I)Im(I)) & E(Im(I)^2) \end{bmatrix}.$$

Since $$E(|I(\omega_i,L)|^2)= E(Re(I)^2) + E(Im(I)^2)$$

and $$E(I^2(\omega_i,L))= E(Re(I)^2) - E(Im(I)^2) + 2jE(Re(I)Im(I)) = 0,$$

it follows that $$E(Re(I)^2) = E(Im(I)^2)$$

and $$E(Re(I)Im(I))= 0.$$

Thus, we have $$E(Re(I)^2) = E(Im(I)^2) = (1/2)E(|I(\omega_i,L)|^2).$$

Defining $$\sigma_I^2 = (1/2)E(|I(\omega_i,L)|^2)$$

we conclude $$\bar{R}_I(\omega_i,L) = \begin{bmatrix} \sigma_I^2 & 0 \\ 0 & \sigma_I^2 \end{bmatrix} = \sigma_I^2 \bar{I}$$

$$\bar{E}(I(\omega_i,L)) = \bar{0}.$$

Thus, we have characterized $I(\omega_i,L)$ as a zero mean, jointly Gaussian two dimensional random variable with covariance matrix given by $\bar{R}_I(\omega_i,L)$. In the next section we will use this characterization of the interference to derive the optimal receiver for the synchronous case.

3.2.3 Optimal Coherent Detector

Using the above characterization of the interference, we can derive the optimal receiver for the synchronous case. Assuming a bit is equally likely to be on or off in channel i, the optimal receiver has the form

$$\frac{f_i(\bar{r}|H_1)}{f_i(\bar{r}|H_o)} \underset{\hat{s}_o}{\overset{\hat{s}_1}{\gtrless}} 1$$

where $f_i(\bar{r}|H_1)$ and $f_i(\bar{r}|H_o)$ are the a posteriori densities for the received signal in channel i given that the transmitted signal was a

one or zero respectivly. For channel i

$$\bar{r}(t|H_1)= Ee^{-\alpha L}\begin{bmatrix}\cos\phi_i\\ \sin\phi_i\end{bmatrix} + \bar{n}(t) + \bar{I}(\omega_i,L)\ ;\ 0\le t \le T$$

$$\hat{r}(t|H_o)= \bar{n}(t) + \bar{I}(\omega_i,L)\ ;\ 0\le t \le T$$

where T is the bit duration and $\bar{n}(t)$ is an additive Gaussian noise characterized by

$$E(\bar{n}(t))= \begin{bmatrix}0\\ 0\end{bmatrix} \quad \text{and} \quad R_n(\tau)= (N_o/2)\delta(\tau)\bar{I}.$$

where $N_o/2$ is the noise level of the local ocillator shot noise.

Also,
$$\bar{I}(\omega_i,L)= \begin{bmatrix}\mathrm{Re}(I(\omega_i,L))\\ \mathrm{Im}(I(\omega_i,L))\end{bmatrix}.$$

After computing the a posteriori densities, we conclude the optimal receiver structure is (Appendix C)

$$\int_0^T \left[r_r(t)\cos\phi_i + r_i(t)\sin\phi_i \right]dt \underset{\hat{s}_o}{\overset{\hat{s}_1}{\gtrless}} (T/2)Ee^{-\alpha L}$$

where $r_r(t)$ and $r_i(t)$ are the real and imaginary parts of the received signal. It is interesting to note that this receiver

structure is the same as for the case where there is no four wave mixing interference. The performance of this receiver is given by

$$Pr(\epsilon)= Q\left[(1/2)Ee^{-\alpha L} \left(\sigma_I^2 + (N_o/2T) \right)^{-1/2} \right].$$

Notice that as $T\rightarrow \infty$

$$Pr(\epsilon) \rightarrow Q\left[Ee^{-\alpha L}/2\sigma_I \right]$$

which means that the performance of the receiver is limited only by the four wave mixing interference. This is because, given a long enough interval of time, we can average out the noise but not the interference (because $I(\omega_i,L)$ is constant over T). As the four wave mixing interference level goes to infinity ($\sigma_I^2 \rightarrow \infty$) $P(\epsilon) \rightarrow 1/2$ because the interference swamps the signal and the best we can do is guess the received signal. Conversely, as the interference goes to zero $Pr(\epsilon)$ goes to its white noise only form as we would expect.

Thus, we have derived the performance of the optimal receiver for a channel corrupted by four wave mixing interference and additive white Gaussian noise caused by the receiver's local oscillator. Because of the structure of the synchronous model these results are worst case for frequency multiplexed systems corrupted by four wave mixing and, as such, set a lower bound on system performance. In later sections we will use these results to determine the performance of the synchronous system as a function of system parameters.

3.3 The General Case

In this section we will extend the previous results to determine the effects of stimulated four wave mixing for a much more realistic system model. As before, we will begin by describing the system model that will be used to determine the characteristics of the four wave interference. Armed with those results, we will then determine the structure and performance of the optimal coherent receiver. Because it is difficult to determine the phase of an optical carrier, we will also examine a noncoherent receiver that assumes no knowledge of the carrier phase. Lastly, we will examine a coherent matched filter receiver and show how its performance almost matches that of the optimal receiver.

3.3.1 Model Description

In this section we will describe a more realistic system model for our four wave mixing analysis (Fig. 16). The system consists of N frequency channels with frequency separation the same as before. However, our signals in each channel are now of the form

$$E(\omega_i, t, L) = \hat{e} E e^{-\alpha L} \sum_{k=-\infty}^{k=\infty} X_{ik} p(t - kT - t_{di}) \cos(\omega_i t - \phi_{ik} - k_i L)$$

where $\{\phi_{ik}\}$ are independent, identically distributed (iid) phase random variables for each pulse, $\{t_{di}\}$ are the iid envelope delay random variables (uniform between -D/2 and D/2 where D goes to infinity), and $\{X_{ik}\}$ are iid random variables to denote the presence or absence of a pulse as before. This model incorporates arbitrary

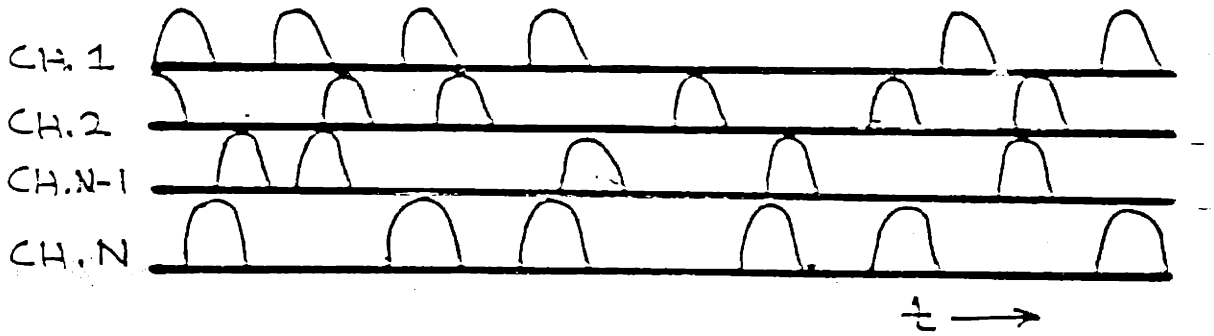

Figure 16

General Case System Model

pulse shapes and assumes the pulse trains in each channel are randomly delayed relative to one another. The phase of the carrier for each pulse is independent. Given this system model, we can now determine the interference and its correlation function.

3.3.2 Characterization of Interference

In this section we will determine the interference given the system model presented in the last section. Again, we will ignore the depletion of the mixing channels and examine the interference terms caused by the crosstalk only.

To facilitate the analysis of $I(\omega_i, L, t)$, we will put our signals in the form

$$\bar{E}(\omega_i, L, t) = \hat{e}\, E_i(L, t) e^{j\omega_i t}$$

$$E_i(L, t) = E e^{-\alpha L}\, e^{-j(k_i - j\alpha)L} \sum_{k=-\infty}^{\infty} e^{j\phi_{ik}}\, p(t - kT - t_{di}).$$

Using our previous results, the envelope of the four wave mixing

interference can be expressed by

$$I(\omega_i,L,t)= Be^{-\alpha L} \sum_a \sum_b \sum_c \frac{\delta(i-(a+b-c))}{(\Delta k_i^2 + 4\alpha^2)^{1/2}} F_i(a,b,c)$$

$$\cdot \left[\sum_{n_a} p(t - n_a T - t_{da}) X_{na} e^{-j\phi_{na}} \right] \left[\sum_{n_b} p(t - n_b T - t_{db}) X_{nb} e^{-j\phi_{nb}} \right]$$

$$\cdot \left[\sum_{n_c} p(t - n_c T - t_{nc}) X_{nc} e^{-j\phi_{nc}} \right]$$

where $F_i(a,b,c)=\exp[j(\tan^{-1}(2\alpha/\Delta k_i)-\Delta k_i L)]e^{-2\alpha L} -\exp[j\tan^{-1}(2\alpha/\Delta k_i)]$ and n_a, n_b, and n_c are summed between $-\infty$ and ∞. As before, the interference is the sum of a large number of random processes. Consequently, we will again assume the interference is a jointly Gaussian random process and, as such, is characterized by it's first and second order moments.

After averaging $I(\omega_i,L,t)$, $I^2(\omega_i,L,t)$, and $I(\omega_i,L,t)I^*(\omega_i,L,t)$ over $\{t_{di}\}$, $\{\phi_{ik}\}$, and $\{X_{ik}\}$, we find the first and second moments of $I(\omega_i,L,t)$ are

$$E(I(\omega_i,L,t))= 0$$

$$E(I(\omega_i,L,t_1)I(\omega_i,L,t_2))= 0$$

$$E(I(\omega_i,L,t_1)I^*(\omega_i,L,t_2))=2\sigma_I^2 \lim_{D\to\infty}\left[\sum_{n=-\infty}^{\infty}(1/D)\int_{-D/2}^{D/2}p(t_1-nT-t_d)p(t_2-nT-t_d)dt_d\right]^3$$

where σ_I^2 is the same as before.

By assuming $|t_1 - t_2| \ll D$, $T \ll D$, and the pulse durations are finite but arbitrarily large, we find the above expected value becomes

$$E(I(\omega_i,L,\tau)I^*(\omega_i,L,0))= 2\sigma_I^2 \left[(1/T)\int_{-\infty}^{\infty} p(-\upsilon + \tau)p(-\upsilon)d\upsilon \right]^3.$$

where $\tau = t_1 - t_2$. For symmetric pulses, this has the form

$$E(I(\omega_i,L,\tau)I^*(\omega_i,L,0))= 2\sigma_I^2 \left[(1/T)\int_{-\infty}^{\infty} p(\tau - \upsilon)p(\upsilon)d\upsilon \right]^3.$$

The above expression is the correlation function of the general case interference. For symmetric pulse shapes, notice the term inside the brackets is just 1/T times the pulse shape convolved with itself. Also, the level of interference is inversely related to the pulse duty cycle- as the pulses are spread further apart in time (i.e. larger T) the interference experienced at any point in time decreases because the probability of having a signal available for mixing in any particular channel decreases. The correlation function

matrix relating the real and imaginary parts of $I(\omega_i, L, t)$ is given by

$$\bar{R}_I(\tau) = \begin{bmatrix} (1/2)E(II^*) & 0 \\ 0 & (1/2)E(II^*) \end{bmatrix} = (1/2)E(II^*)\ \bar{I}.$$

Thus, we have characterized the four wave mixing interference for the general case as a zero mean, jointly Gaussian stationary noise. Using this characterization, we will be able to determine the optimal detector for the general case.

3.3.3 Detection Issues for the General Case

As we have shown, stimulated four wave mixing can be modeled as an additive colored Gaussian noise. Given that, our system in any particular channel consists of a communication channel that corrupts our signal with an additive interference and with white noise caused by the shot noise from the local oscillator of our receiver. This detection problem is unique because the characteristics of the interference are dependent on the system parameters (p(t), $\Delta\omega$, N, etc.). Consequently, if the system parameters are changed, so is the interference. Thus, to get some insight into the effects of four wave mixing interference, we will examine the effects of four wave mixing on a system that uses a particular p(t). Because of its analytic characteristics, we will examine a system where p(t) is a sinc pulse (Fig. 17).

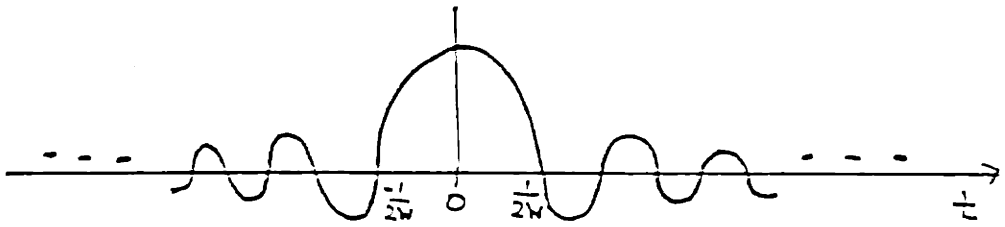

Figure 17

Sinc Pulse

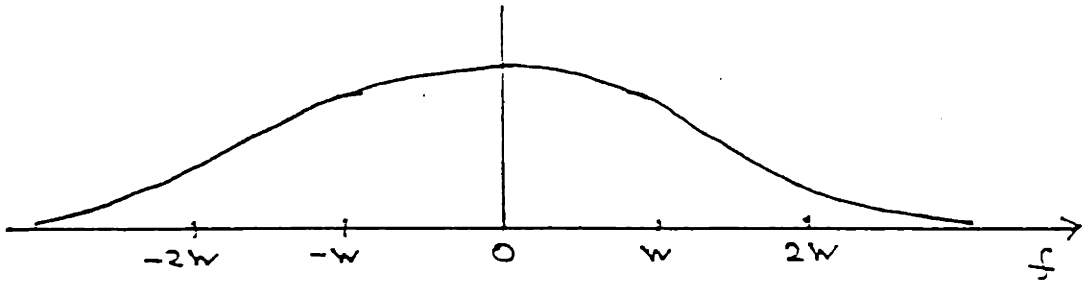

Figure 18

Interference Power Spectrum Using Sinc Pulse

In the following sections, we will concentrate on deriving the structure and performance of optimal and suboptimal single-shot receivers. By single-shot we mean the receivers are designed for detecting a single isolated pulse. In reality, though, we are trying to detect a pulse embedded within a stream of pulses. Hence, there might be other effects such as intersymbol interference that must be taken into consideration. We will show in later sections how using a suboptimal receiver structure and properly choosing p(t) can eliminate intersymbol interference.

3.3.4 Optimal Coherent Detector Structure and Performance

In this section we present the structure and derive the performance of the optimal detector for a system corrupted by four wave mixing interference assuming knowledge of the signal carrier phase, ϕ_i. Our procedure will be to first derive the correlation function for p(t). This will then be used to determine the optimal receiver structure and performance as a function of the system parameters.

This is a binary detection problem where we are trying to distinguish which of two signals was transmitted. The transmitted signals (assuming knowledge of the carrier phases) are

$$\bar{s}_1(t) = Ee^{-\alpha L}\, p(t) \begin{bmatrix} \cos\phi_i \\ \sin\phi_i \end{bmatrix}$$

$$\bar{s}_o(t) = \bar{0}.$$

The received signals, given that a one or a zero was transmitted, are

$$\bar{r}_i(t|H_1) = \bar{s}_1(t) + \bar{I}(\omega_i, L, t) + \bar{n}(t)$$

$$\bar{r}_i(t|H_o) = \bar{I}(\omega_i, L, t) + \bar{n}(t)$$

here $\bar{n}(t)$ is the same as defined in the synchronous case.

Our first step is to determine the correlation function matrix, $\bar{R}_I(\tau)$, for our particular p(t). The p(t) we will use is a sinc pulse of the form (Fig. 17)

$$p(t) = \sin(2\pi Wt) \; / \; \pi t$$

where W is the bandwidth of the pulse's spectrum. Using this and our expression for the correlation function of a symmetric pulse

$$\bar{R}_I(\tau) = R_I(\tau)\bar{I}$$

$$R_I(\tau) = (2\sigma_I^2/T^3) \; [\; p(\tau) * p(\tau) \;]^3$$

we can derive $R_I(\tau)$ for the sinc pulse. First we define

$$h(\tau) = p(\tau) * p(\tau)$$

$$h(\tau) \leftrightarrow H(f)$$

and

$$p(\tau) \leftrightarrow P(f)$$

where $H(f)$ and $P(f)$ are the fourier transforms of $h(\tau)$ and $p(\tau)$ respectivly. Using the fact that

$$R_I(\tau) = (2\sigma_I^2/T^3)h^3(\tau)$$

$$P(f) = \begin{cases} 1 & ; -W \leq f \leq W \\ 0 & ; \text{otherwise} \end{cases}$$

and $$H(f) = P^2(f)$$

we find that

$$H(f) = \begin{cases} 1 & ; -W \leq f \leq W \\ 0 & ; \text{otherwise} \end{cases},$$

$$h(\tau) = \sin(2\pi W\tau)/\pi\tau \ .$$

Plugging into the expression for $R_I(\tau)$ we conclude

$$R_I(\tau) = (2\sigma_I^2/T^3)[\ \sin(2\pi W\tau)/\pi\tau\ ]^3$$

Now that we have an expression for the correlation function, we will derive it's corresponding power spectrum which is defined by

$$R_I(\tau) \leftrightarrow S_I(f).$$

We know that

$$S_I(f) = (2\sigma_I^2/T^3)[\ P(f)*P(f)*P(f)\ ].$$

After convolving P(f) with itself three fold we determine that

$$S_I(f) = (2\sigma_I^2/T^3) \cdot \begin{cases} (1/2)(f+3W)^2 & ; -3W \le f \le -W \\ 3W^2 - f^2 & ; -W \le f \le W \\ (1/2)(-f+3W)^2 & ; W \le f \le 3W \\ 0 & ; \text{otherwise} \end{cases} .$$

Thus, we now have expressions for the correlation function and power spectrum of the interference assuming p(t) is a sinc pulse. The power spectrum is depicted in Fig. 18.

Using the correlation function and power spectrum of the interference, we can now find the performance of the optimal receiver. For equiprobable signals, the structure of the optimal receiver is given by

[Van Trees]

$$\int_{-\infty}^{\infty}\int \bar{r}_i^{\dagger}(t)\ \bar{Q}_I(t-u)\ \bar{s}_1(u)\ dtdu - (1/2)\int_{-\infty}^{\infty}\int \bar{s}_1^{\dagger}(t)\ \bar{Q}_I(t-u)\ \bar{s}_1(u)\ dtdu \underset{\hat{s}_o}{\overset{\hat{s}_1}{\gtrless}} 0$$

where the inverse kernel, $\bar{Q}_I(t)$, is chosen such that

$$\int_{-\infty}^{\infty} \bar{R}_I(t-u)\ \bar{Q}_I(u-z)\ du = \delta(t-z)\bar{I}.$$

The performance of this receiver is given by

$$P(\epsilon) = Q(d/2)$$

where $$d^2 = \int\int \bar{s}_1^{\dagger}(t)\ \bar{Q}_I(t-u)\ \bar{s}_1(u)\ dtdu.$$

In order to evaluate $P(\epsilon)$ we must determine $\bar{Q}_I(t)$. Assuming a long observation interval, the Fourier transform of $\bar{Q}_I(t)$, $S_q(f)$, is the inverse of the power spectrum of the noise plus the interference [Van Trees]. In other terms

$$\bar{I}(\omega_i, z, t) \text{ has power spectrum } \bar{S}_I(f)$$

$$\bar{n}(t) \text{ has power spectrum } \bar{S}_n(f)$$

then $$\bar{S}_q(f) = [\ \bar{S}_I(f) + \bar{S}_n(f)\ ]^{-1} = S_q(f)\bar{I}.$$

and $$\bar{Q}_I(\tau) = Q_I(\tau)\bar{I}$$

To determine the performance metric, we put d^2 in the form

$$d^2 = \int_{-\infty}^{\infty} p(t)q(t)dt$$

$$\text{where } q(t) = \int_{-\infty}^{\infty} Q_I(t-s)p(s)ds$$

which is just the convolution of $Q_I(t)$ and $p(t)$. Defining the Fourier transform of $q(t)$ as

$$q(t) \longleftrightarrow Q(f)$$

we know that

$$Q(f) = \begin{cases} S_q(f) & ; -W \leq f \leq W \\ 0 & ; \text{otherwise} \end{cases}$$

therefore

$$Q(f) = \begin{cases} \left[(N_o/2) + (2\sigma_I^2/T^3)(3W^3 - f^2) \right]^{-1} & ; -W \leq f \leq W \\ 0 & ; \text{otherwise} \end{cases}.$$

Using Parseval's theorem,

$$d^2 = \int_{-\infty}^{\infty} p(t)q(t)dt = \int_{-\infty}^{\infty} P(f)Q(f)df.$$

Thus, $$d^2 = \int_{-W}^{W} (E^2 e^{-2\alpha L})\left[(N_o/2) + (2\sigma_I^2/T^3)(3W^2 - f^2) \right]^{-1} df \ .$$

Solving this integral we find

$$d^2 = \frac{E^2 T^3 e^{-2\alpha L}}{2\sigma_I^2 \psi} \ln\left[\frac{|W+\psi|}{|W-\psi|} \right] .$$

$$\text{where } \psi = \left[(N_o T^3/4\sigma_I^2) + 3W^2 \right]^{1/2} .$$

As a check of the result we see that

$$\lim_{\sigma_I^2 \to 0} d^2 = (4W/N_o) E^2 e^{-2\alpha L}$$

$$\lim_{\sigma_I^2 \to \infty} d^2 = 0.$$

Thus, as $\sigma_I^2 \to 0$, d^2 goes to it's white noise only value as it must. Also, as $\sigma_I^2 \to \infty$, d^2 goes to zero because the signal is totally swamped by the interference. Also, as the pulse duty cycle decreases (increasing T) d^2 goes to it's white noise only value because the interference level goes to zero. Finally, we see that d^2 decreases with increasing W because of the increased white noise energy level associated with the greater bandwidth.

3.3.5 Single-Shot Noncoherent Detector

The optimal detector derived in the previous section assumed knowledge of the carrier phase. However, estimating the carrier phase of an optical carrier can be quite complicated. It seems desirable, therefore, to know how well a noncoherent receiver performs relative to the optimal coherent receiver. As before the transmitted signals are of the form

$$\bar{s}_1(t) = Ee^{-\alpha L}\, p(t) \begin{bmatrix} \cos\phi \\ \sin\phi \end{bmatrix}$$

$$\bar{s}_o(t) = \bar{0}$$

where ϕ is uniformily distributed between $-\pi$ and π and each signal is equally likely to be transmitted. From [Van Trees] we know the likelyhood function for the random phase case has the form

$$\Omega[\bar{r}(t)] = \int_{-\infty}^{\infty} p(\phi)\, \exp[\, L_c\cos\phi + L_s\sin\phi - (1/2)d^2\,]d\phi$$

where $$r(t) = \begin{bmatrix} r_r(t) \\ r_I(t) \end{bmatrix},$$

$p(\phi)$ is the probability distribution for ϕ , d^2 is defined as before,

$$L_c = Ee^{-\alpha L} \int_{-\infty}^{\infty}\int r_r(t)Q_I(t-\mu)p(\mu)dtd\mu \ ,$$

$$L_s = Ee^{-\alpha L} \int_{-\infty}^{\infty}\int r_I(t)Q_I(t-\mu)p(\mu)dtd\mu \ ,$$

and $Q_I(t-\mu)$ is the inverse kernel from the last section. Plugging in our $p(\phi)$ we see that

$$\Omega[\bar{r}(t)] = (1/2\pi) \int_{-\pi}^{\pi} \exp[\ L_c\cos\phi + L_s\sin\phi - (1/2)d^2\ ]d\phi \ .$$

Solving this integral we find

$$\Omega[\bar{r}(t)] = e^{-d^2/2}\ I_o[\ (L_c^2 + L_s^2)^{1/2}\ ]$$

where $I_o(x)$ is a zero-order modified Bessel function of the first kind. The corresponding decision rule for our noncoherent receiver is

$$I_o[\ (L_c^2 + L_s^2)^{1/2}\ ] \underset{\hat{H}_o}{\overset{\hat{H}_1}{\gtrless}} e^{d^2/2}$$

By using the fact that $I_o(x)$ is a monotonic function and modifying the threshold we can simplify the receiver structure to yield

$$L_c^2 + L_s^2 \underset{\hat{H}_o}{\overset{\hat{H}_1}{\gtrless}} \tau .$$

Arthurs and Dym [Arthurs] showed the average probability of error for such a system assuming a bit is equally likely to be on or off is bounded by

$$Pr(\epsilon) \geq (1/2)e^{-d^2/8}$$

where d^2 is the same as in the previous section. To compare this with the average probability of error for the optimal receiver we note that, for small probabilities of error, we can express the optimal $Pr(\epsilon)$ as

$$Pr(\epsilon) = Q(d/2) \approx (2/d)(2\pi)^{-1/2}\, e^{-d^2/8}.$$

Thus, as we already knew, the coherent receiver always performs better than the noncoherent receiver. For large signal to noise ratios (i.e. large d^2), this difference in performance is very small.

3.3.6 Structure and Performance of a Matched Filter Receiver

Looking at Fig. 18, we see that the power spectrum of the interference in the signal passband is almost flat. Consequently, we would expect a matched filter detector that assumes the interference is white in the passband would perform almost as well as the optimal receiver. In contrast to the optimal single shot receiver, the matched filter receiver does not induce intersymbol interference for the sinc pulse. Also, the matched filter is less complicated than the optimal receiver. It is interesting, therefore, to find out how the performance of such a receiver compares to the optimal. We will start by deriving the performance of a coherent matched filter receiver. Then we will compare it's performance to that of the optimal receiver.

The matched filter receiver we will analyze is shown in Fig. 19. The response of the matched filter is

$$\bar{H}(t)= \left[\; h_1(t) \quad h_2(t) \; \right]$$

where $$h_1(t)= Ee^{-\alpha L}p(t)\cos\phi$$

and $$h_2(t)= Ee^{-\alpha L}p(t)\sin\phi$$

because p(t) is symmetric. Thus, the outputs of the matched filter, given $s_o(t)$ or $s_1(t)$ was sent, are

$$r^{\circ}(t|H_1)= s^{\circ}(t) + N^{\circ}(t)$$

$$r^{\circ}(t|H_o)= N^{\circ}(t)$$

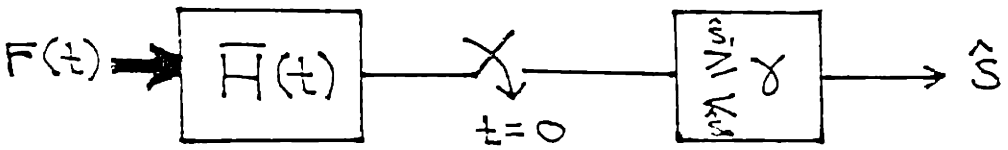

Figure 19

Matched Filter Receiver

where $s^{\circ}(t)= Ee^{-\alpha L}p(t)*p(t)[\ \cos^2\phi + \sin^2\phi\ ] = E^2e^{-2\alpha L}\ p(t)$

and similarly, $N^{\circ}(t)= [\ I(t)+n(t)\ ]*Ee^{-\alpha L}p(t)$.

It is easy to show that $N^{\circ}(t)$ is a zero mean Gaussian random process with it's power spectrum given by

$$S_o(f)= (\ S_I(f) + (N_o/2)\ )E^2e^{-2\alpha L}|P(f)|^2\ .$$

Plugging in our expressions for $S_I(f)$ and $P(f)$ (remember $p(t)$ is a sinc pulse), it is clear that

$$S_o(f)= \begin{cases} (2E^2e^{-2\alpha L}\sigma_I^2/T^3)(3W^2-f^2) + (N_o/2)E^2e^{-2\alpha L} & ;\ -W \le f \le W \\ 0 & ;\ \text{otherwise} \end{cases}$$

After sampling $r^{\circ}(t)$, we get the sufficient statistic r which is a Gaussian random variable characterized by

$$f(r|H_1)= N(m_r\ ,\ \sigma_r^2\ )$$

$$f(r|H_o)= N(0\ ,\ \sigma_r^2\ )$$

where $$m_r= E^2e^{-2\alpha L}p(t)*p(t)\Big|_{t=0} = 2WE^2e^{-2\alpha L}$$

$$\sigma_r^2= \int_{-W}^{W} S_o(f)df\ = E^2e^{-2\alpha L}[\ (32\sigma_I^2W^3/3T^3) + N_oW\ ].$$

Thus, the detection problem can be viewed as a binary detection problem. Assuming that H_1 and H_o are equally likely, the threshold setting should be

$$\gamma = E^2 W e^{-2\alpha L}.$$

From this we get the average probability of error

$$Pr(\epsilon) = Q\left(EWe^{-\alpha L}\left[(32W^3\sigma_I^2/3T^3) + N_o W \right]^{-1/2} \right).$$

Now that we have an expression for the $Pr(\epsilon)$ for the matched filter receiver, we need to compare it's performance with that of the optimal receiver. This is accomplished by examining the ratio of the arguments of the Q functions. In other terms, given

$$Pr(\epsilon) = Q(d_o/2) \; ; \text{ for optimal receiver}$$

$$Pr(\epsilon) = Q(d_m/2) \; ; \text{ for matched filter receiver}$$

define $$\text{ratio} = d_o/d_m .$$

If the performance of the two receivers are approximately the same, we would expect ratio to be near 1 for all expected combinations of system parameters. Conversely, if the optimal receiver performs much better than the matched filter receiver, we expect the ratio to be large.

From this and the previous section we know that

$$d_o^2 = (E^2T^3e^{-2\alpha L}/2\psi\sigma_I^2)\ \ln\left[\frac{|W+\psi|}{|W-\psi|}\right]$$

$$\text{where } \psi = \left[\ (N_oT^3/4\sigma_I^2) + 3W^2\ \right]^{1/2}$$

and

$$d_m^2 = \frac{4E^2W^2e^{-2\alpha L}}{(32W^3\sigma_I^2/3T^3) + N_oW}\ .$$

Taking the ratio of these two quantities we conclude

$$\text{ratio}^2 = \left[\frac{(16W^2/3) + (T^3N_o/2\sigma_I^2)}{4\psi W}\right]\ln\left[\frac{|W+\psi|}{|W-\psi|}\right]$$

This ratio can be expressed in terms of the dimensionless parameter

$$\eta = E_w\ /\ E_I$$

where E_w is the energy of the white shot noise in the passband and E_I is the energy of the interference in the passband. We will express the ratio in terms of this parameter.

To that end we note that

$$E_I = \int_{-W}^{W} S_I(f)df = 32\sigma_I^2W^3/3T^3$$

and likewise, $$E_w = N_o W$$

Therefore $$\eta = 3N_o T^3/32\sigma_I^2 W^2 .$$

Expressing ratio^2 in terms of η we conclude

$$\text{ratio}^2 = \frac{(4/3)(1+(\eta/2))}{[(4/3)\eta+3]^{1/2}} \ln \left[\left| \frac{1+ [(4/3)\eta+3]^{1/2}}{1- [(4/3)\eta+3]^{1/2}} \right| \right] .$$

Thus, we have expressed the ratio of the performance parameters in terms of the dimensionless parameter η.

In order to compare the performance of the two receivers, we will look at ratio for the worst case scenario $E_I >> E_w$ ($\eta \to 0$) where we would expect the difference in performance to be greatest. It is easy to show that

$$\lim_{\eta \to 0} \text{ratio} = 1.007 .$$

This means that regardless of whether the white noise or the interference dominates, the performance of the two receivers are virtually identical. This is because the power spectrum of the interference looks "almost white" over the signal passband. It is reasonable to assume that, for any other pulse shape that results in an interference power spectrum that is almost white over the signal passband, the matched filter detector will perform almost as well as the optimal detector. Also, because the matched filter detector does

not cause intersymbol interference among adjacent pulses and is less complex, it is more desirable than the optimal single shot detector.

3.4 Discussion of Results

In this section, the theory developed thus far is used to determine the effects of stimulated four wave mixing on the performance of frequency multiplexed communication systems in single mode optical fiber. We will start by examining the fundamental limits that phase matching imposes upon four wave mixing. Then, once that ground work is laid, we will examine the relationship between the communication system characteristics (numbers of channels, input powers, length of fiber, etc.) and the performance degradation caused by stimulated four wave mixing.

3.4.1 Effect of Phase Matching on Interference

As previously stated, the interference level is very sensitive to the degree of phase matching among the frequency channels. We found that, even for small amounts of fiber dispersion, the interference levels are negligible because of poor phase matching. This occurs only when the channels are very closely spaced or the fiber dispersion is very low.

From our previous analysis, we know that the level of interference in the i^{th} channel due to four wave mixing is expressed

by its correlation function

$$E(I(\omega_i,L,\tau)I^*(\omega_i,L,0))= (2\sigma_I^2/T^3)\left[\int_{-\infty}^{\infty} p(-\upsilon + \tau)p(-\upsilon)d\upsilon \right]^3$$

$$\sigma_I^2 = \beta^3 e^{-2\alpha L} \sum_a \sum_b \sum_c \frac{\delta(i-(a+b-c))}{\Delta k_i^2 + 4\alpha^2} \left[1+ e^{-4\alpha L} -2e^{-2\alpha L} \cos\Delta k_i L \right]$$

where β is a physical constant, $\Delta k_i = k_a+k_b-k_c-k_i$, and a,b,c are summed between 1 and N except i. Notice that each term in the sum for σ_I^2 is dependent on it's Δk_i. When all Δk_i are equal to zero (phase matched) σ_I^2 is maximized and grows monotonically with the number of channels. When the Δk_i are not equal to zero, σ_I^2 saturates at fairly small values of N. In fig. 20 σ_I^2 is plotted versus N for the worst case channel. Notice that, even for small dispersion levels (3.0ps/km-nm) and channel spacing (5.0Ghz.), σ_I^2 saturates at about N=120. This is because, as more channels are added to the system, the additional three-tuples that mix are increasingly further apart in frequency and, therefore, are increasingly poorly phase matched. Each additional mixing term then contributes less and less to σ_I^2; leading to saturation. Thus, we conclude that four wave mixing is only a factor when the phase matching is extremely good. For that reason, our results will examine the case where we have perfect phase matching.

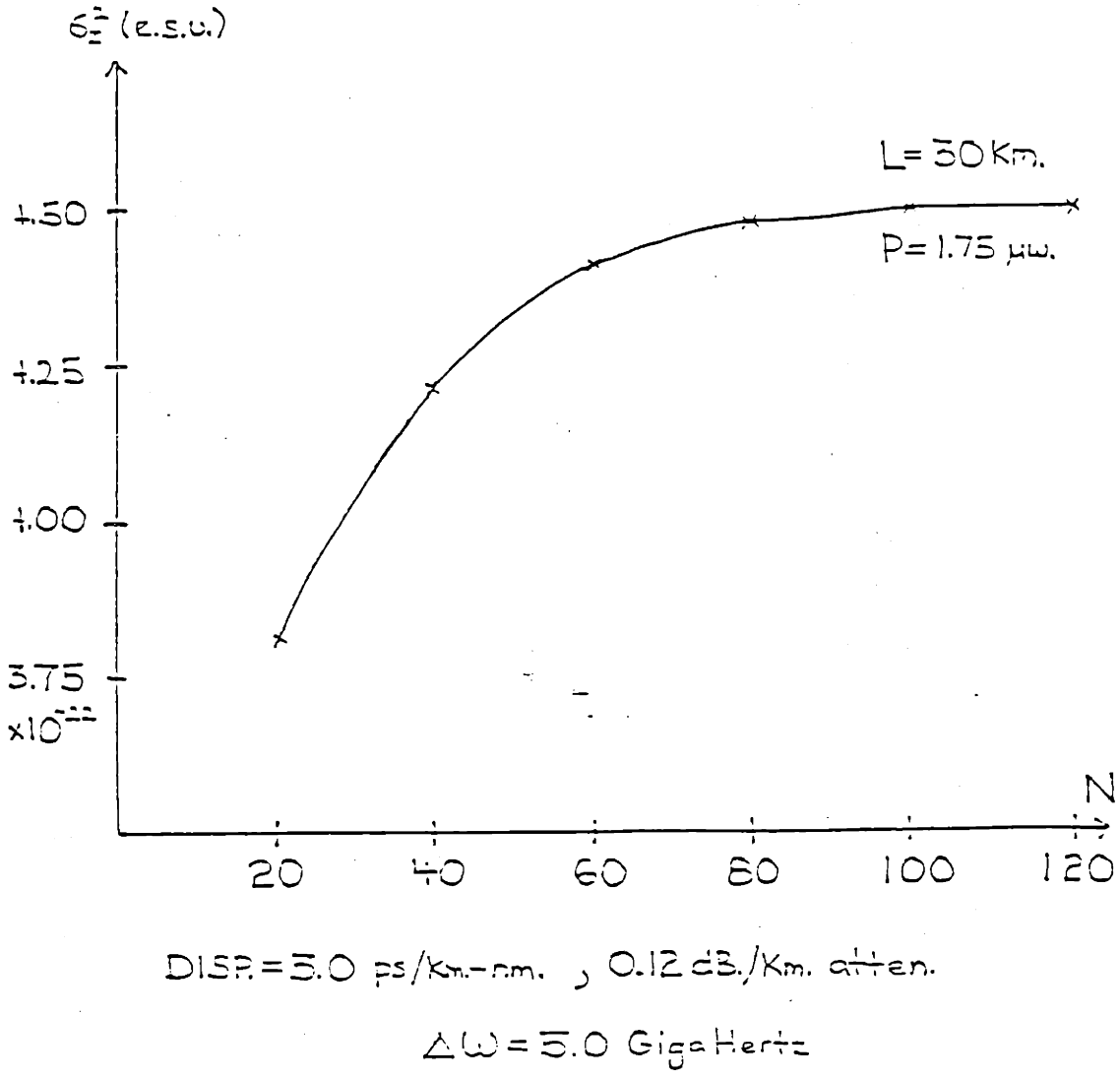

Figure 20

Saturation of σ_I^2 in Non-Phase-Matched System

3.4.2 Effect of Fiber Length and Number of Channels

Here we examine how four wave mixing interference affects performance for systems with various lengths of fiber and numbers of channels. To facilitate this, we plotted the performance using the results developed from the analysis. For each length of fiber, we set the peak input field amplitude, E, such that $Pr(\epsilon)=10^{-9}$ given that the signal is corrupted by the white shot noise only. Then, for each length of fiber we examined $Pr(\epsilon)$ in the worst case channel for various N assuming the frequency channels are perfectly phase matched.

For the synchronous case, we plotted the results in Fig. 21 and Fig. 22. Notice that the performance degradation is most sensitive to the fiber length. This is because of the longer interaction lengths and because we must increase the initial peak field amplitude as the fiber length increases in order to meet our power budget. Notice also that, at long fiber lengths, the performance degradation is more sensitive to the number of channels. This is due to each additional mixing term being larger due to the higher average input powers and interaction lengths.

If we plot $Pr(\epsilon)$ versus N for the general case using the sinc pulse, we get similar results (Fig. 23, Fig. 24). Notice, even though we set E so that $Pr(\epsilon)=10^{-9}$ for each L, the general case performance is better than the synchronous case. This is expected because the general case model allows asynchronism among the pulses in each channel; resulting in decreased levels of interference.

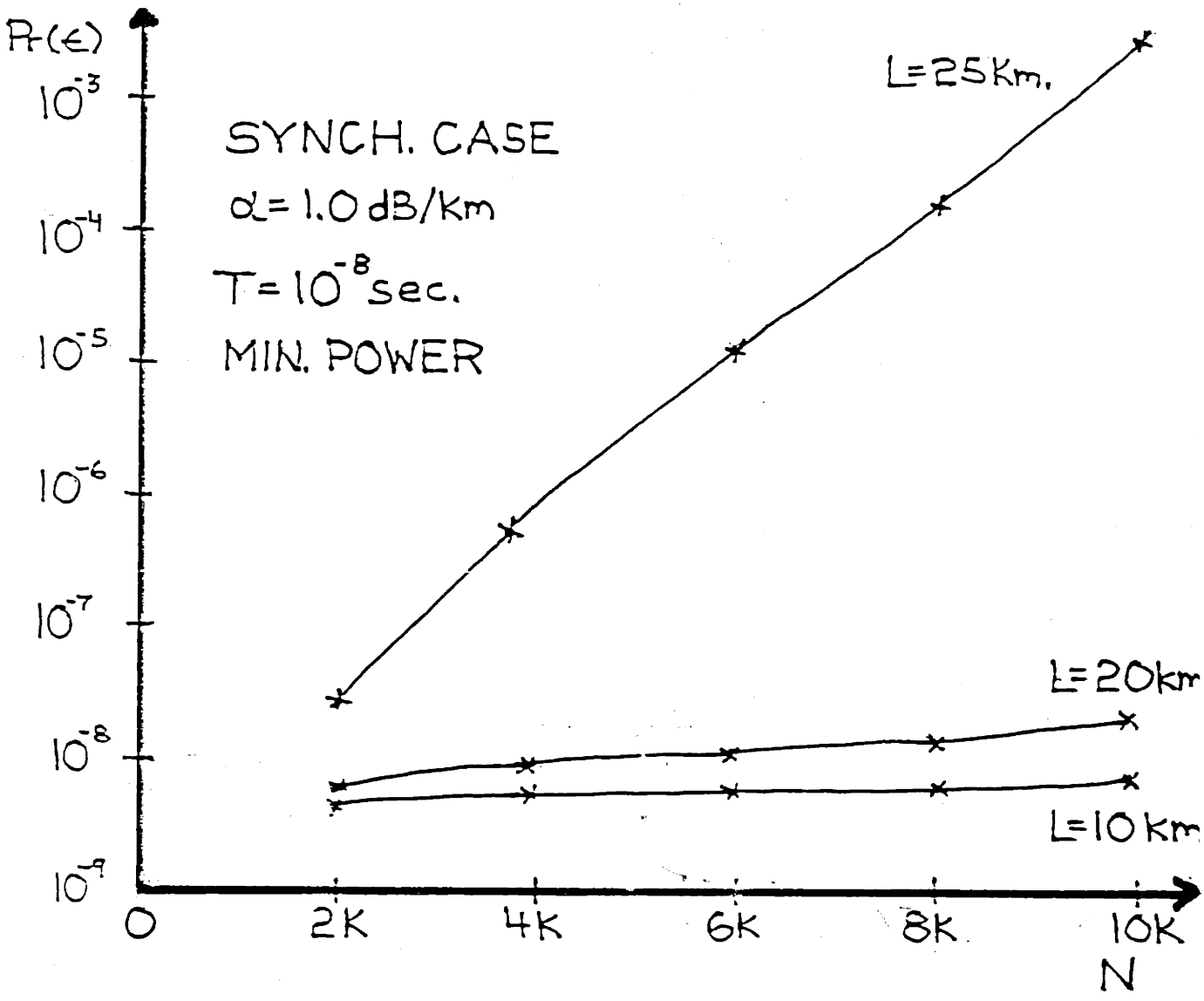

Figure 21

Pr(ϵ) vs. N for Synchronous Case

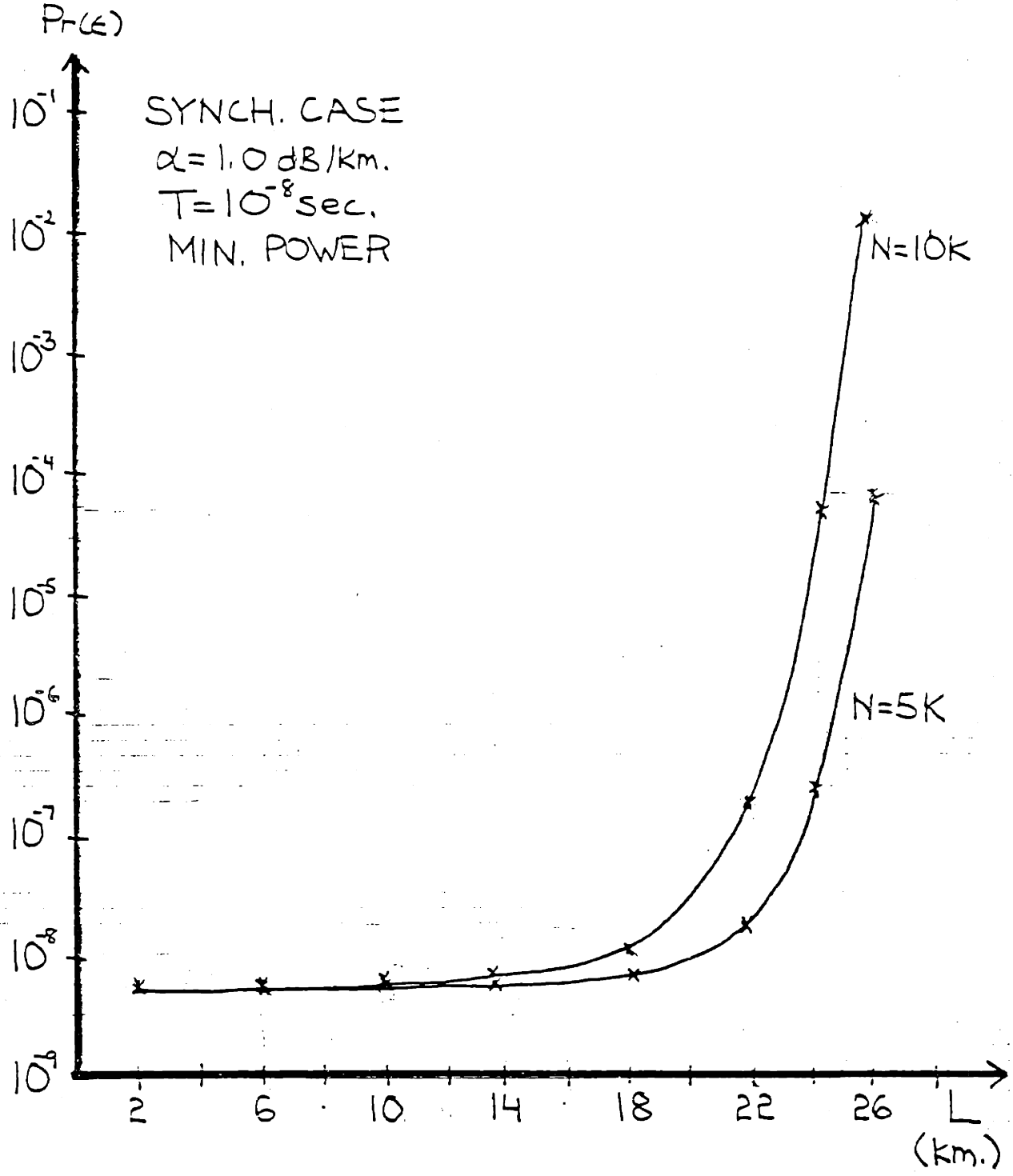

Figure 22

Pr(ε) vs. L for Synchronous Case

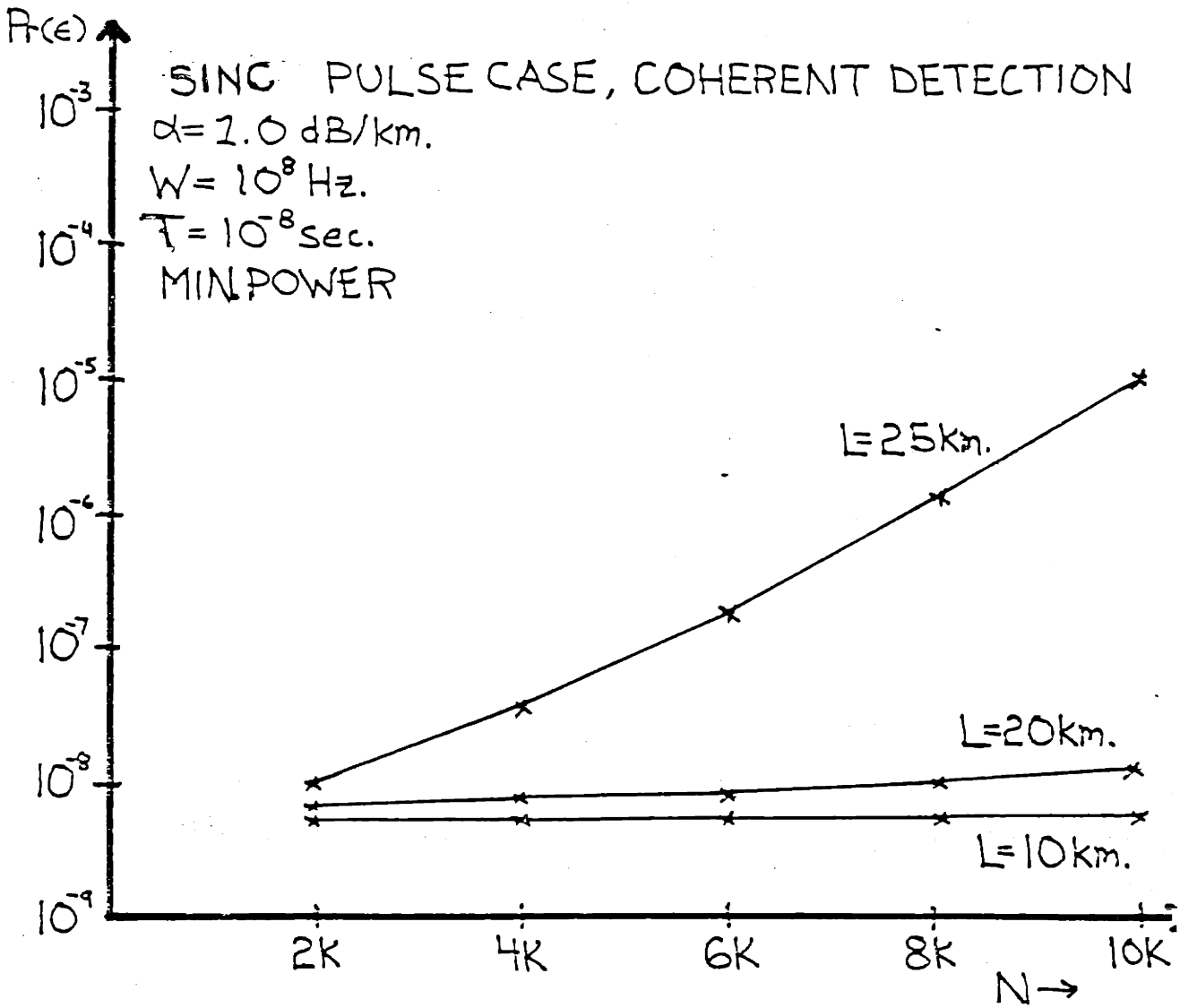

Figure 23

Pr(ϵ) vs. N for General Case

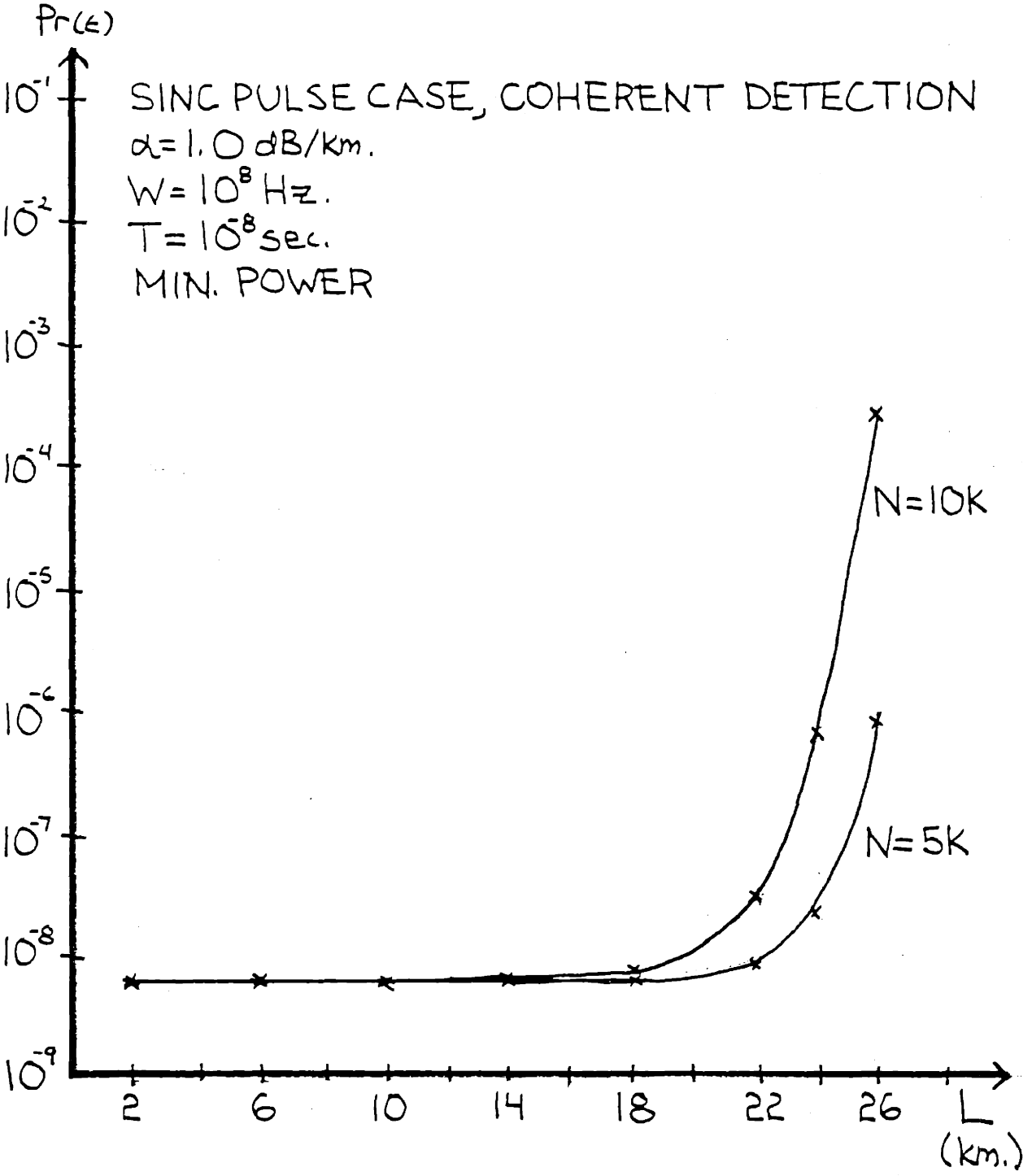

Figure 24

Pr(ε) vs. L for General Case

The calculations were performed assuming E was set to yield $Pr(\epsilon)=10^{-9}$ assuming no four wave mixing interference. The corresponding average powers were relatively low (approximately 10^{-8}W.) Consequently, we plotted the performance using average input powers scaled to reflect more realistic scenarios. The results given that the average powers have been doubled are shown in Fig. 25 and Fig. 26. $Pr(\epsilon)$ is lower for short fiber lengths because the interaction length is not long enough for the interference to accumulate. But, as the fiber length increases the interference eventually swamps the signal. As we go to even higher average powers the effect of fiber length is even more pronounced (Fig. 27).

3.4.3 Effect of Pulse Spacing on Interference

For the general case the interference level varies with $1/T^3$ where T is the pulse spacing. Thus, if we lower the pulse duty cycle (while keeping the energy per pulse constant) we should see an improvement in performance corresponding to decreased interference. To illustrate that we plotted $Pr(\epsilon)$ for various values of T in Fig. 28. As expected, the performance improved as we increased the spacing between pulses while maintaining constant pulse widths. However, this improvement comes at the expense of slower data rates.

3.4.4 Comparison of Coherent and Noncoherent Receivers

Plotted in Fig. 29 is the performance of the coherent and noncoherent receivers for the general case. As expected, their performances are almost identical for large signal to noise ratios. However, as the signal to noise ratio decreases (manifested by

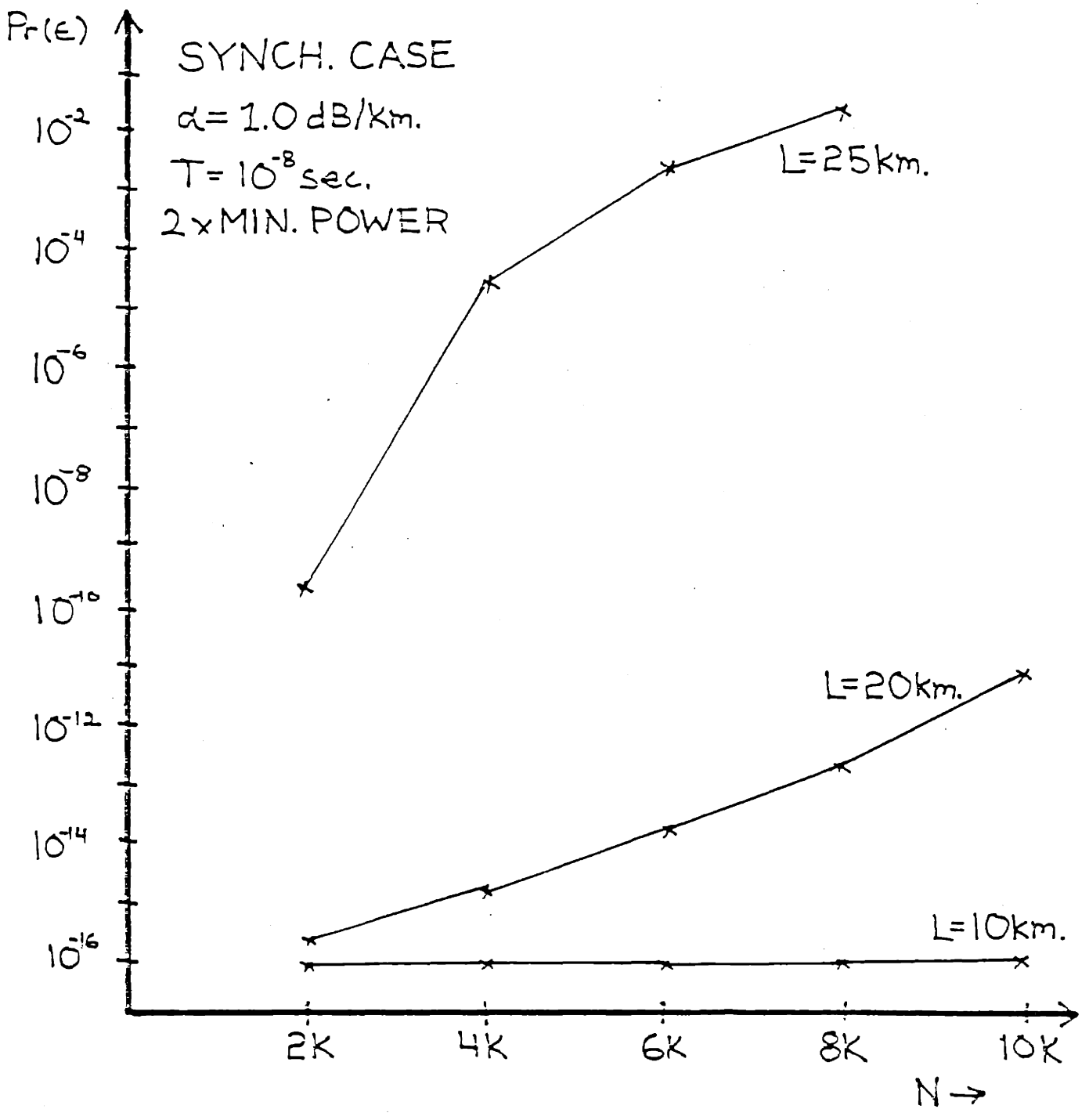

Figure 25

Pr(ε) vs. N for Synchronous Case, 2x Minimum Power

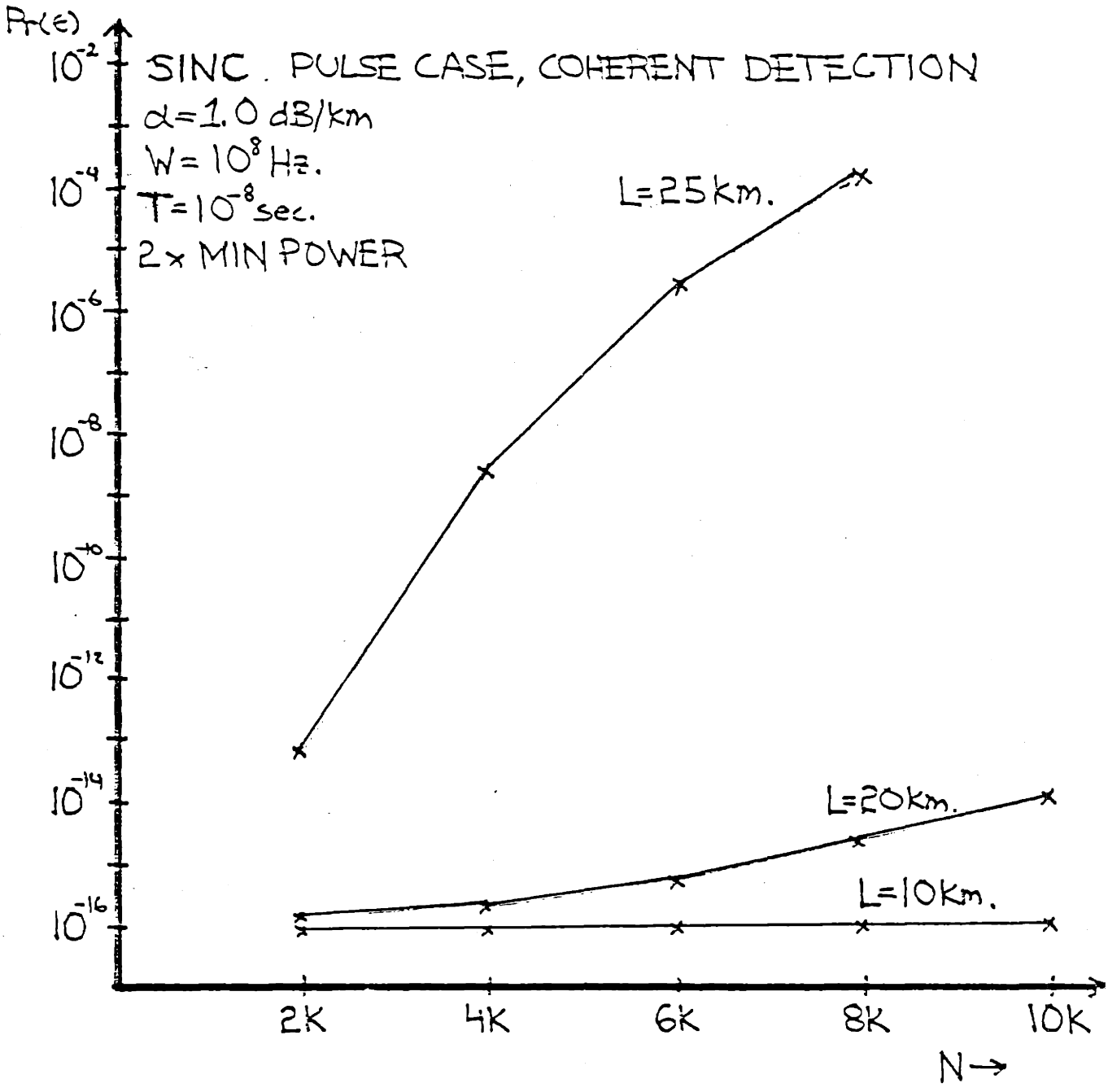

Figure 26

Pr(ϵ) vs. N for General Case, 2x Minimum Power

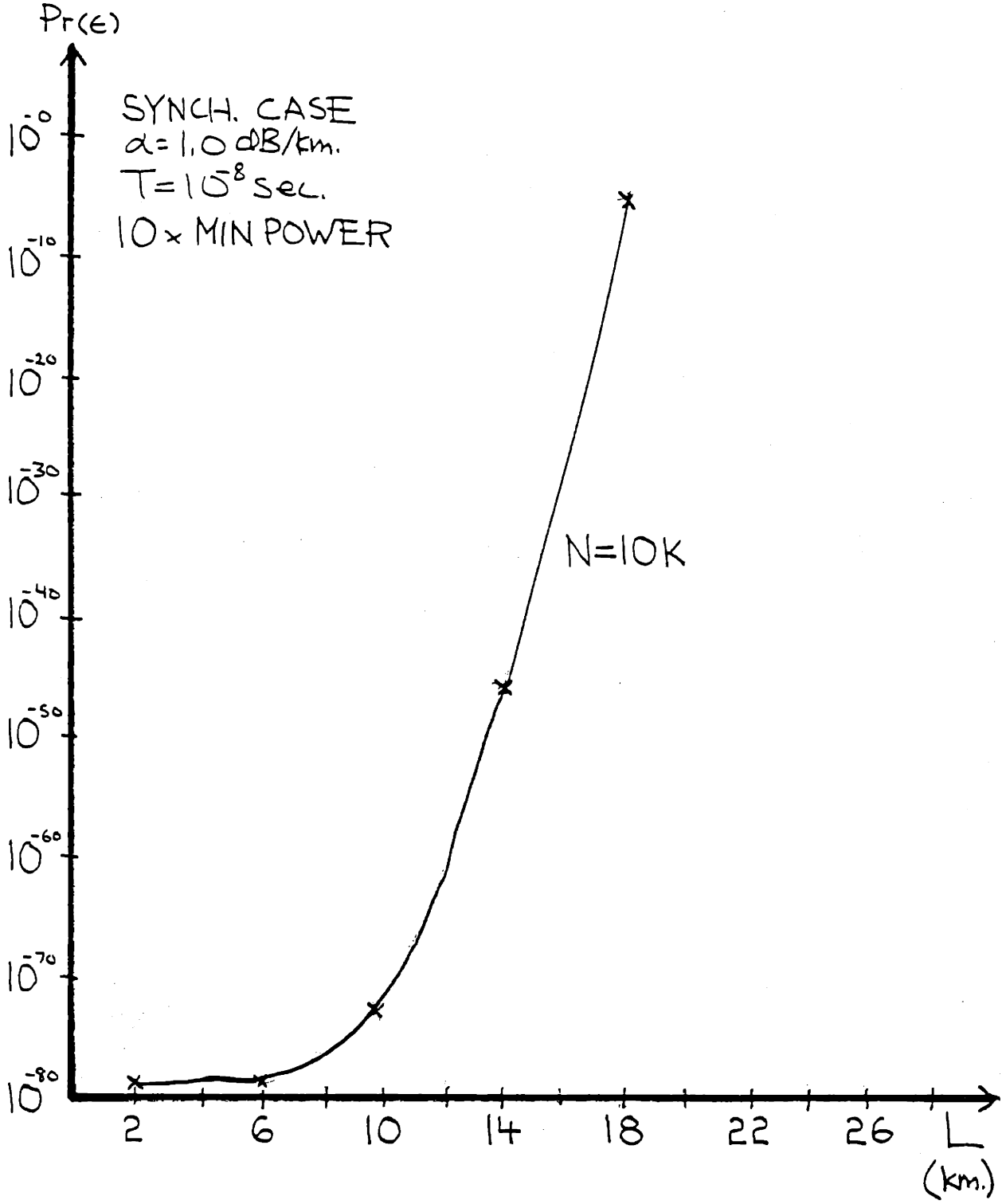

Figure 27

Pr(ϵ) vs. L for Synchronous Case, 10x Minimum Power

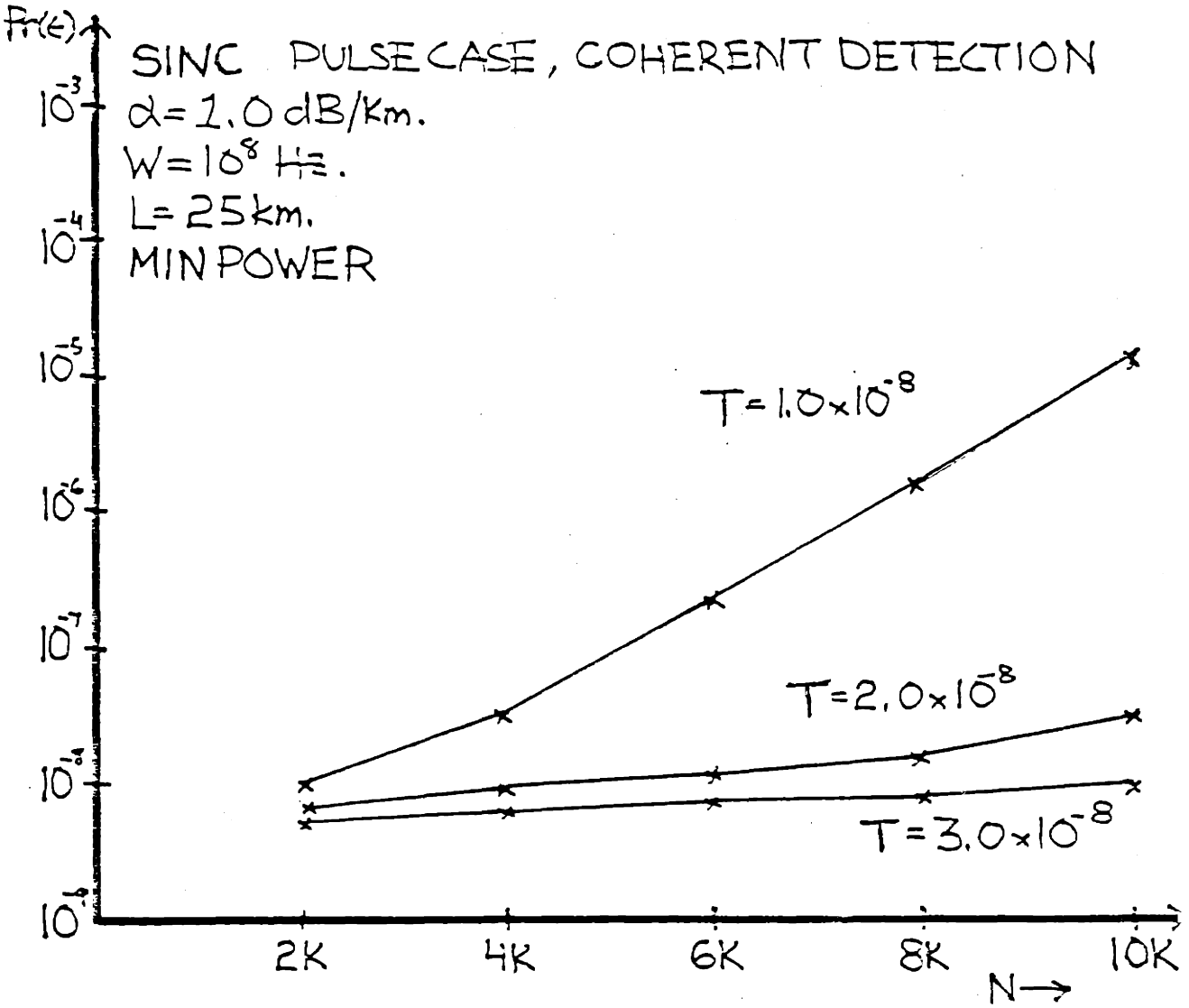

Figure 28

Effects of Changing Pulse Duty Cycle for General Case

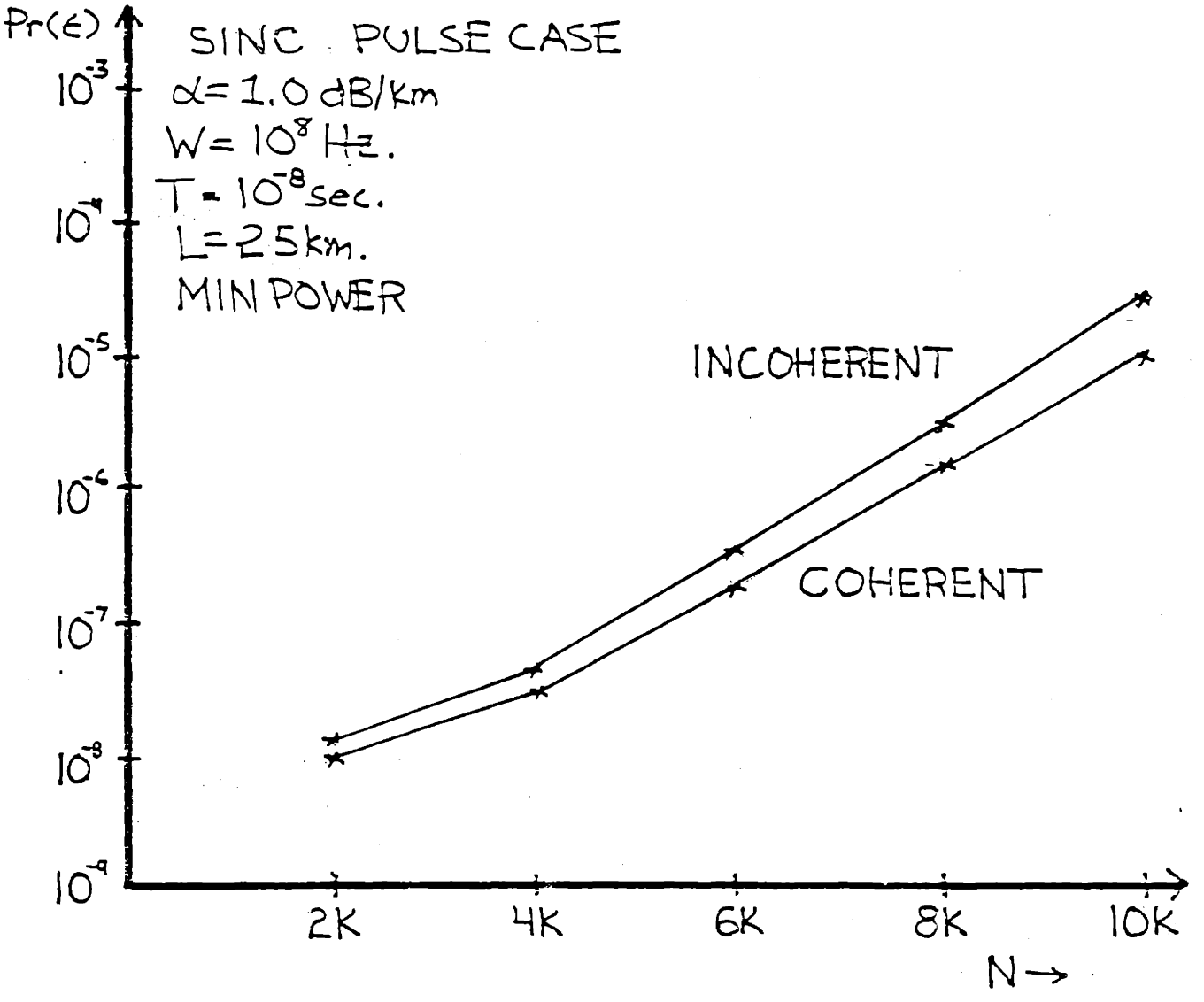

Figure 29

Comparison of Coherent and Noncoherent Receivers

increasing $Pr(\epsilon)$), the performance of the two receivers spreads futher apart. For the scenarios envisioned, the added performance gains derived from using coherent detection may not outweigh the added complexity of the receiver.

3.5 Conclusions

Based on the above data it seems that stimulated four wave mixing will not be a factor in networks with link lengths less than approximatly 10km. irrespective of the number of channels. For longer fiber lengths it is possible that four wave mixing can cause unacceptable levels of interference. However, remember the above numerical results were for phase matched systems. If the fiber is dispersive, four wave mixing interference levels are severely reduced. Therefore, for most foreseeable scenarios, stimulated four wave mixing will not be a factor.

IV The Effects of Stimulated Raman Scattering on FDM Systems

In this chapter we will analyze the effects of stimulated Raman scattering on frequency multiplexed systems utilizing single mode optical fiber. As with four wave mixing, our emphasis will be on analyzing the communication performance of the systems instead of more physical measures such as the level of depletion. Stimulated Raman scattering can be considered to be a random fade that scales the signal powers. Given that, our task is to statistically describe this fading and determine the optimal receiver structure and performance.

Section 4.1 describes the model that will be used to examine on-off keying systems. Section 4.2 uses the physics of stimulated Raman scattering to describe the fading while section 4.3 describes the receiver for on-off keying and determines it's performance. Finally, numerical results will be presented in section 4.4.

4.1 System Model

For the Raman analysis we will use the synchronous case system model where we assume rectangular pulse shapes and slotted channels. As before, we have an N channel frequency multiplexed system where the carrier frequency of each channel is given by

$$\omega_i = i\Delta\omega + \omega_o$$

where ω_o is the center of the band and $\Delta\omega$ is the channel frequency separation. The signals in any particular time slot in channel i can be described as

$$\bar{E}(\omega_i,L,t)= \hat{e}E(\omega_i,L)e^{j\omega_i t}$$

$$E(\omega_i,L)= X_i\ e^{-j(k_i-j\alpha)L}$$

where L is the fiber length, α is the fiber attenuation coefficient, k_i is the propagation constant for channel i, and $\{X_i\}$ are independent, identically distributed modulation random variables that are one with probability P and zero with probability 1-P. We have not included the carrier phase in the expression for $E(\omega_i,L)$ because stimulated Raman scattering does not depend upon phase. We will use the envelopes of the signals, $E(\omega_i,L)$, without loss of generality.

4.2 Characterization of Raman Fading in Worst Case Channel

Using the system model we can describe the effect of stimulated Raman scattering on frequency multiplexed systems in single mode fiber. As mentioned in chapter II, stimulated Raman scattering in single mode fiber transfers power from the higher freqency signals to the lower frequency signals. As a consequence, the highest frequency channel will experience the worst fading; it is the performance bottleneck. Therefore, we will examine the fading experienced by the highest frequency channel.

The differential equation that describes the effects of stimulated Raman scattering on the worst case channel, N, is

$$\frac{dE(\omega_N,L)}{dL} + \alpha E(\omega_N,L) = -E(\omega_N,L)(P(0)e^{-\alpha L}/A_{eff}) \sum_i \gamma_i X_i$$

where $$E(\omega_N,L)= E(L)e^{-\alpha L} ,$$

i is summed from 1 to N-1, and $E(\omega_N,L)$ is the signal in the N^{th} channel, A_{eff} is the effective cross sectional area of the fiber, P(0) is the initial signal power, and γ_i is the Raman coupling coefficient between channels N and i. Plugging the expression for $E(\omega_N,L)$ into the differential equation we find

$$\frac{dE(L)}{dL} = -E(L)(P(0)e^{-\alpha L}/A_{eff}) \sum_i \gamma_i X_i .$$

Solving this expression we see

$$E(L)= C \exp[(P(0)e^{-\alpha L}/A_{eff}\alpha) \sum_i \gamma_i X_i].$$

Using the initial condition $E(\omega_n,L=0)= E(0)$ we finally conclude

$$E(\omega_N,L)= E(0)e^{-\alpha L} \exp[-(L_{eff}P(0)/A_{eff}) \sum_i \gamma_i X_i]$$

where $L_{eff}= (1-e^{-\alpha L})/\alpha$ and $P(0)= A_{eff}E^2(0)/2\eta$

Notice the stimulated Raman scattering scales the signal by an exponential "fade factor" that is dependent on the fiber length (L_{eff}), the signal intensities ($P(0)/A_{eff}$), and the number and frequency spacing of the channels ($\sum \gamma_i X_i$);

$$G(L)= \exp[\ -(L_{eff}P(0)/A_{eff}) \sum_i \gamma_i X_i\ ]$$

Also notice that G(L) is constant over the pulse duration and decays with L. Our next task is to determine the statistics of the received signal, $E(\omega_N,L)$, when it is scaled by this Raman fading factor.

The sum in the exponent of the fade factor,

$$X = \sum \gamma_i X_i\ ,$$

is the sum of a large number of iid random variables. Therefore, using the DeMoivre-Laplace theorem we can assume X is Gaussian distributed. In other terms

$$f(X)= N(\ E(X),\ \sigma_x^2\ )$$

$$E(X)= P \sum_i \gamma_i \qquad \text{and} \qquad \sigma_x^2 = (P-P^2)\sum_i \gamma_i^2\ .$$

Thus,

$$E(\omega_N,L)= E(0)e^{-\alpha L}\ \exp[\ -(L_{eff}P(0)/A_{eff})X\ ].$$

It can be shown that $E(\omega_N,L)$ is log-normally distributed (Appendix D) with

$$f(E(\omega_N,L))= [E(\omega_N,L)(\sigma_x P(0)L_{eff}/A_{eff})(2\pi)^{1/2}\ ]^{-1}$$

$$\cdot\exp\left[\ \frac{-[\ \ln[E(\omega_N,L)] - \ln[E(0)] + \alpha L + (E(X)L_{eff}P(0)/A_{eff})\ ]^2}{2(\sigma_x^2\ L_{eff}P(0)/A_{eff})^2}\ \right]$$

$$E(E(\omega_N,L))= E(0)e^{-\alpha L}\exp[\ -(E(X)L_{eff}P(0)/A_{eff}) + (\sigma_x^2\ L_{eff}P(0)/A_{eff})^2\ ]$$

and $$\sigma_E^2 = E^2(0)e^{-2\alpha L}\ (\ \exp[(\sigma_x^2\ L_{eff}P(0)/A_{eff})^2] - 1)$$

$$\cdot\exp(\ (\sigma_x^2\ L_{eff}P(0)/A_{eff})^2 - 2(E(X)L_{eff}P(0)/A_{eff})\ )$$

As expected, the average value of the faded signal is the original signal times an exponential factor that decays with L. As a sanity check, we see that

$$\lim_{P(0)\to 0} E(E(\omega_N,L)) = E(0)e^{-\alpha L}$$

and

$$\lim_{P(0)\to 0} \sigma_E^2 = 0$$

which means that the signal in the worst case channel experiences no Raman fading when there are no signals launched in the lower frequency channels. As a final check, notice that when we set the probability of pulses being present in the lower frequency channels

to zero (equivalently, set E(X) and σ_x^2 to zero) the mean and varience of the faded signal go to the above values- as we would expect.

4.3 The Optimal Receiver Structure and Performance

Now that we have characterized the effects of the Raman scattering, we must develop the optimal receiver for an on-off modulated signal in the presence of constant log-normal fading. This problem has been addressed Halme [Halme 69] and others in the context of atmospheric optical communications. Unfortunately, although the structure of the optimal receiver can be readily determined, it's performance cannot be calculated analytically. Instead, suboptimal structures and bounds on performance were obtained for several special cases. Because we are primarily interested in the effects of stimulated Raman scattering rather than solving this general problem, we will resort to examining the performance of an idealized receiver structure.

To get some insight into the receiver structure we will use, let's examine the structure of this detection problem. Essentially it is a binary detection problem where the distance between the means of the two a posteriori densities is random (Fig. 30). The received signal is of the form

$$\bar{r}(t)= E(0)G(L)e^{-\alpha L}\begin{bmatrix}\cos\phi_N\\ \sin\phi_N\end{bmatrix} + \bar{n}(t) \quad ; \; H_1 \text{ transmitted}$$

$$\bar{r}(t)= \bar{n}(t) \quad ; \; H_o \text{ transmitted}$$

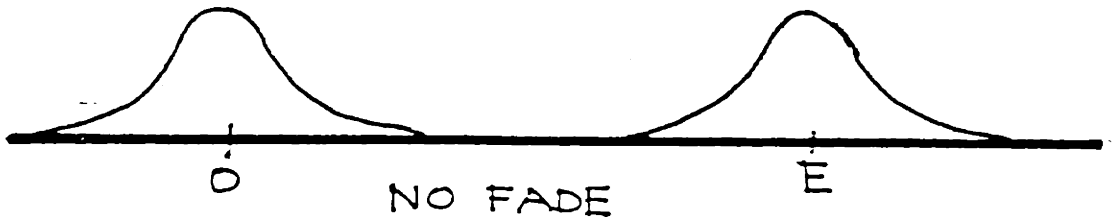

Figure 30

Raman Fading

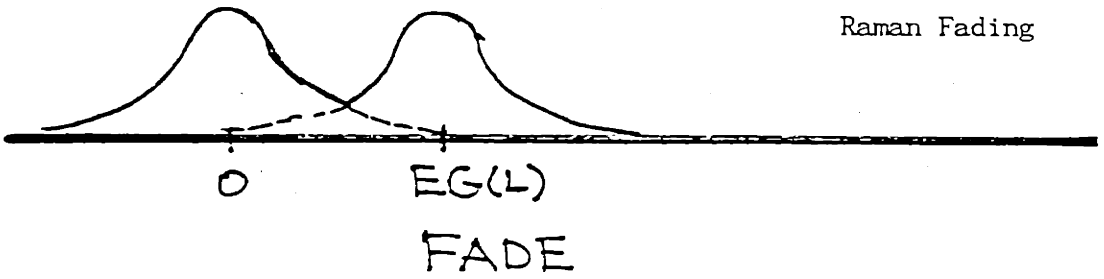

Figure 31

Raman Fading in High SNR Systems

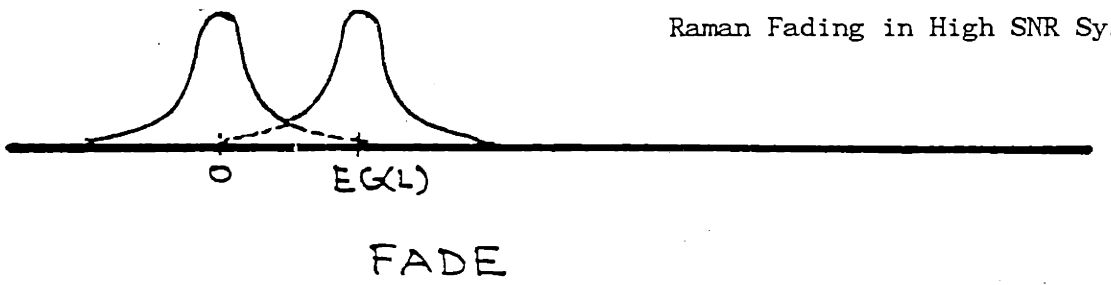

where $\bar{n}(t)$ is a white, jointly Gaussian noise with

$$R_n(\tau) = (N_o/2)\delta(\tau)\bar{I}$$

The optimal receiver selects a decision boundary such that the average probability of error is minimized. The average probability of error can be expressed by

$$Pr(\epsilon) = P_o Pr(\hat{H}_1 | H_0) + P_1 Pr(\hat{H}_o | H_1).$$

If the decision boundary is set too high, $Pr(\hat{H}_o | H_1)$ will be large. But, on the other hand, if the decision boundary is set too low $Pr(\hat{H}_1 | H_o)$ will be large. Thus, the optimal boundary must strike a balance between these two extremes. If we assume the distance between the means (i.e. pulse energy) of the a posteriori densities is large compared to the standard deviation of the white noise, the average probability of error due to the white noise is significant only when the fading is severe (Fig. 31). Thus, when the white noise level is small compared to the pulse energy, it is useful to measure performance in terms of the probability that the fade is severe enough to cause the probability of error due to the white noise to exceed some threshold. We will use this performance measure.

The receiver we will use for our analysis has the form

$$\int_0^T r_r(t)\cos\phi_N + r_I(t)\sin\phi_N \, dt \underset{\hat{H}_0}{\overset{\hat{H}_1}{\gtrless}} (1/2)E(0)TG(L)e^{-\alpha L}.$$

This is just the form of the optimal coherent receiver assuming that we know the value of the fade parameter, G(L). This means that, for every value of G(L), the receiver will pick the optimal decision boundary. The performance of this receiver is better than any fixed boundary structure but it is still can give us some insight into the effects of stimulated Raman scattering.

We want to find the probability that the fade is severe enough to cause the error probability due to the white noise to exceed 10^{-6}. In order to accomplish this, we must find the values of G(L) such that

$$Pr(\epsilon|G(L)) \geq 10^{-6}$$

where $Pr(\epsilon|G(L))$ is the average probability of error given G(L). From chapter III we know

$$Pr(\epsilon|G(L)) = Q\left((1/2)E(0)G(L)e^{-\alpha L}(N_o/2T)^{-1/2} \right).$$

For $$Pr(\epsilon|G(L)) \geq 10^{-6}$$

we know that

$$(1/2)E(0)G(L)e^{-\alpha L}(N_o/2T)^{-1/2} \leq 5$$

or, in other terms

$$G(L) \leq \frac{10e^{\alpha L}}{E(0)} (N_o/2T)^{1/2}$$

$$G(L)= \exp(-(L_{eff}P(0)/A_{eff})X).$$

Using the two expressions above we determine that, in order for $Pr(\epsilon|G(L)) \geq 10^{-6}$ we must satisfy

$$X \geq \upsilon$$

where $\upsilon= -(A_{eff}/L_{eff}P(0))(\alpha L + \ln[(10/E(0))(N_o/2T)^{1/2}])$

and X is the Gaussian random variable.

Thus we conclude

$$[\% \text{ time } Pr(\epsilon)\geq 10^{-6}] = Q[(\upsilon-E(X))/\sigma_x].$$

Using this performance metric, we can determine under which conditions the Raman fade is deep enough to cause significant degradation in the system performance.

4.4 Discussion of Results

Using the performance metric derived in the last section we can begin to determine the effects of stimulated Raman scattering on frequency multiplexed systems. We begin by calculating the performance of the worst case channel for various fiber lengths and numbers of channels. As before, we set the average input powers for each length of fiber to yield $Pr(\epsilon)=10^{-9}$ in the absence of Raman scattering. Remembering that

$$[\ \%\ \text{time}\ Pr(\epsilon) \geq 10^{-6}\ ] = Q(Z)$$

where

$$Z = (\upsilon - E(x))/\sigma_x$$

we plot $\log_{10}(Q(Z))$ versus the number of channels for families of L in Fig. 32. Notice that the chances of having a fade deep enough to cause $Pr(\epsilon)\geq 10^{-6}$ are practically nil. This is because the powers needed to yield $Pr(\epsilon)=10^{-9}$ in the absence of Raman fading are too small (10^{-8} Watts) to stimulate significant Raman interaction. We can see why this is true by examining the Raman fade factor

$$G(L)= \exp\ [\ -(L_{eff}P(0)/A_{eff}) \sum_j \tau_j X_j\ ]$$

The exponent is very small because the values of τ_j range from 0 to 6×10^{-19} and the signal intensities are not very large for the scenarios we have considered. The only way the exponent of the Raman

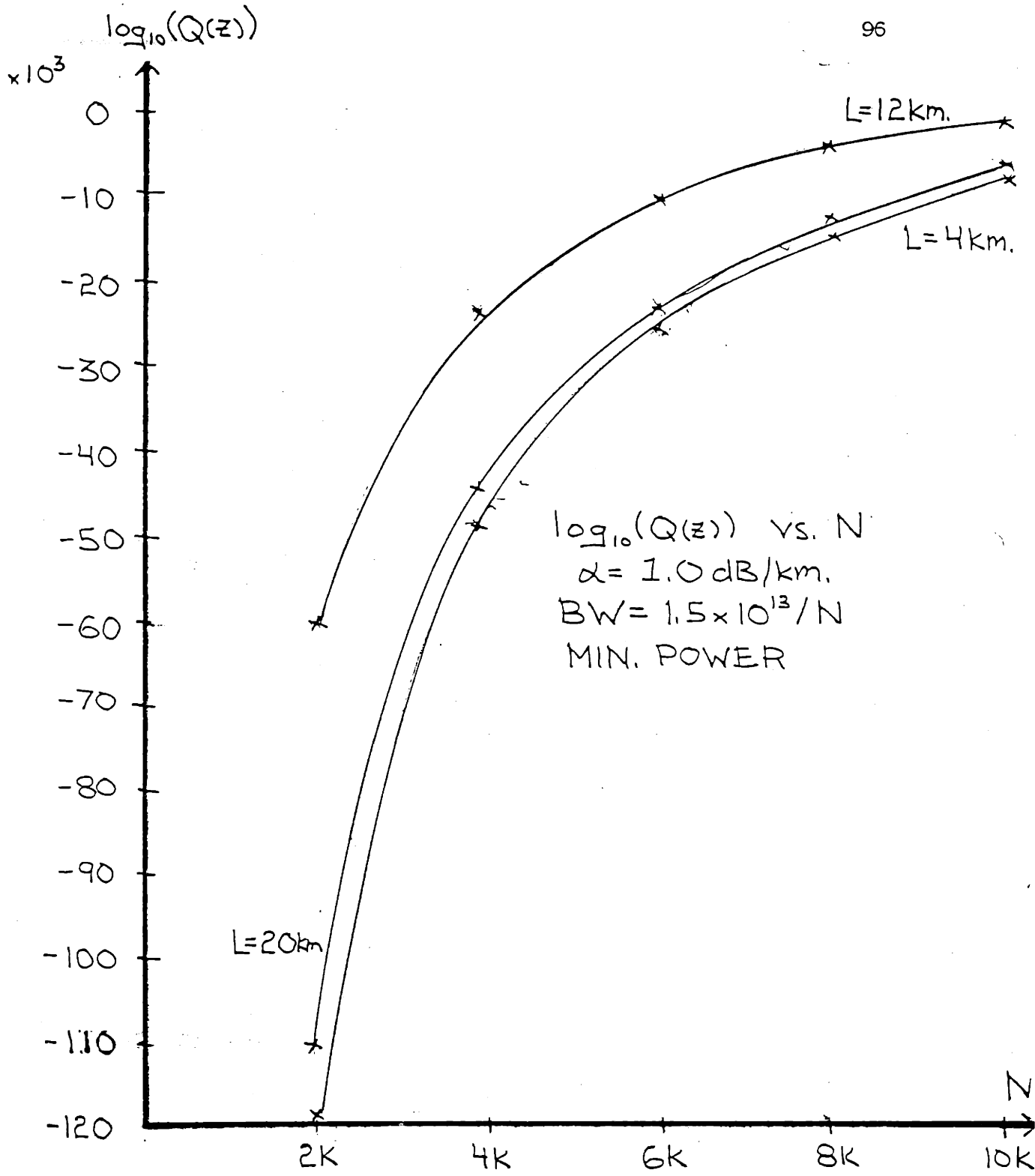

Figure 32

Performance in Presence of Raman Fading, Minimum Power

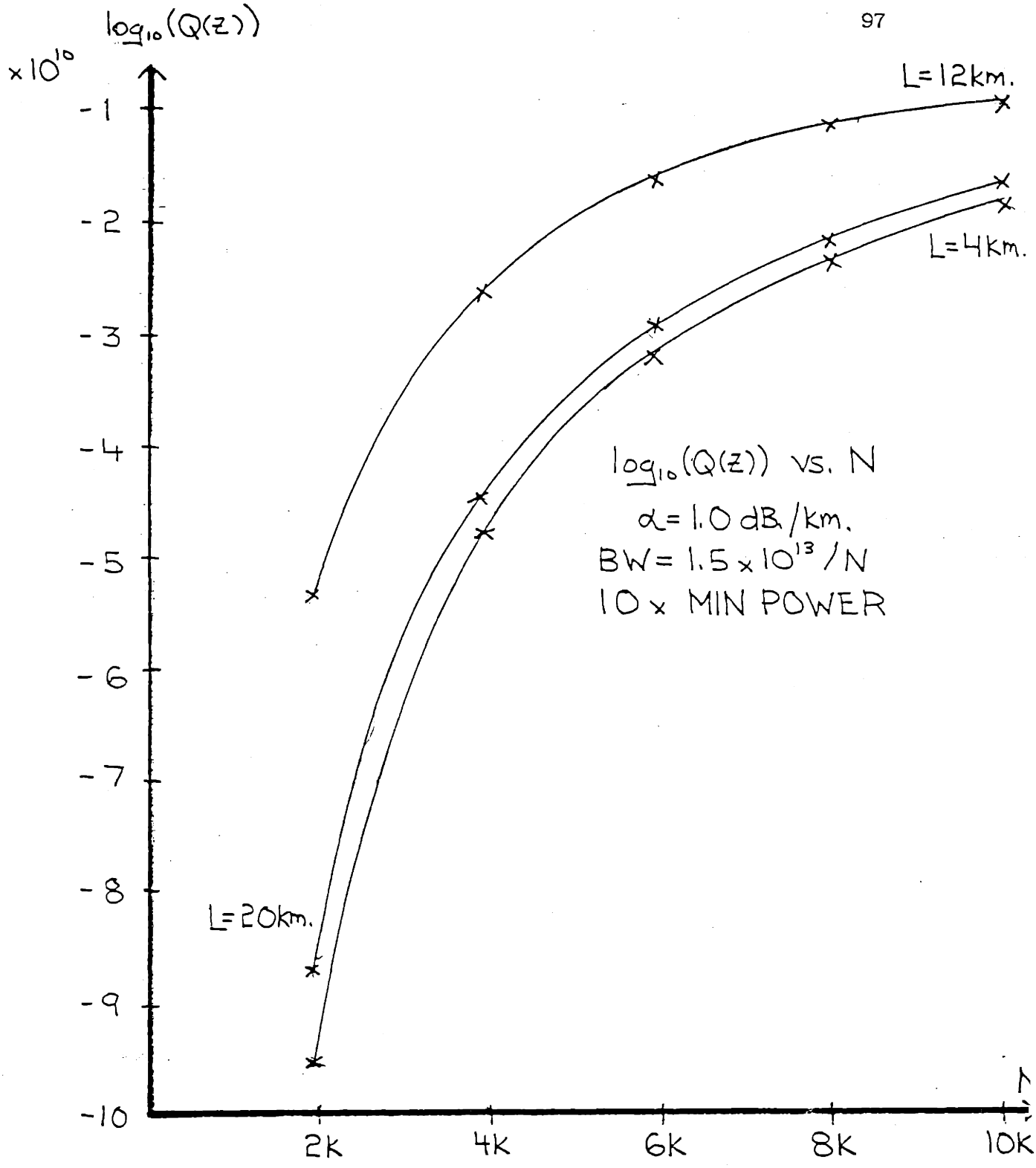

Figure 33

Performance in Presence of Raman Fading, 10x Minimum Power

gain factor could be large is for the initial intensity to be larger (increase P(0) or decrease A_{eff}) or use fiber with a larger Raman gain profile.

Next, we tried increasing the input powers to see if that would have any significant effect on the system performance. In Fig. 33 we plotted $\log_{10}(Q(Z))$ versus N for various families of L where we have increased the powers by a factor of 10. Notice that the chances of a deep fade decreased as the signal powers were increased. This is because, as the signal powers are increased, the signal to noise ratio increases much faster than the fading.

For both plots, the chances of experiencing a deep fade peaked for some length of fiber then decreased for longer fiber lengths. This because the Raman fading was weak enough such that fiber attenuation overshadowed the chances of fading for long fiber lengths.

4.5 Conclusions

The overwhelming conclusion of this analysis is that stimulated Raman scattering is not significant for the scenarios we have examined. Thus, for fiber lengths $\leq$25km. and large numbers of channels, we do not have to worry about Raman scattering. This was because the Raman interaction is very weak for the signal powers that would realistically be used with frequency multiplexed systems that use large numbers of channels.

V Conclusion

5.1 Research Results

In this thesis we have analytically determined the effects of stimulated four wave mixing and stimulated Raman scattering on large scale frequency multiplexed communication systems employing single mode optical fiber. The overwhelming conclusion of the results were that the effects of the nonlinearities are negligible for fiber lengths $\leq$ 10km. For longer fiber lengths ($\geq$25km.), four wave mixing may cause unacceptable interference while Raman scattering will probably be negligible.

5.2 Future Research

Throughout the research we examined the effects of the nonlinearities on point to point links utilizing frequency multiplexing. However, frequency multiplexing will most likely be considered for use in networks. Therefore, it is necessary to determine the effects on these nonlinearities frequency multiplexed systems in networks. Several characteristics of networks that may require analysis are:

* **Topology**. Even though a network may serve a small geographic area, the interaction lengths might be long due to the network topology. Consequently, some topologies might be susceptable to intolerable levels of four wave mixing interference.

* **Optical amplifiers.** The use of optical amplifiers may increase the nonlinear effects by boosting the signal powers and possibly by nonlinear interaction within the amplifiers themselves.

* **Couplers** The use of couplers in networks may either enhance or diminish the effects of the nonlinearities by combining and splitting signals.

These issues should be addressed if the results of this thesis are to be extended to optical networks employing frequency multiplexing.

Appendix A

Derivation of $E(|I(\omega_i,L)|^2)$

Here we derive $E(|I(\omega_i,L)|^2)$ for the synchronized pulse case. Since

$$E(|I(\omega_i,L)|^2)= E(I(\omega_i,L)I^*(\omega_i,L))$$

we must start by finding I^*. This is easy if we put I in exponential form;

$$I(\omega_i,L) =B \sum_a \sum_b \sum_c \frac{e^{-\alpha L} X_a X_b X_c \delta(i-(a+b-c))}{(\Delta k_i^2 + 4\alpha^2)^{1/2}}$$

$$\cdot\left[e^{j[\mathrm{Tan}^{-1}(2\alpha/\Delta k_i)+\Delta\phi_i -\Delta k_i L]} e^{-2\alpha L} - e^{j[\mathrm{Tan}^{-1}(2\alpha/\Delta k_i) +\Delta\phi_i]} \right].$$

Using this, the expression for $I^*(\omega_i,L)$ becomes

$$I^*(\omega_i,L)=B \sum_a \sum_b \sum_c \frac{e^{-\alpha L} X_a X_b X_c \delta(i-(a+b-c))}{(\Delta k_i^2 + 4\alpha^2)^{1/2}}$$

$$\cdot\left[e^{-j[\mathrm{Tan}^{-1}(2\alpha/\Delta k_i)+\Delta\phi_i -\Delta k_i L]} e^{-2\alpha L} - e^{-j[\mathrm{Tan}^{-1}(2\alpha/\Delta k_i) + \Delta\phi_i]} \right].$$

When we take the expectation of II^* the only nonzero terms will be those such that the $\{\phi_i\}$ cancel. This is a result of

$$\int_{-\pi}^{\pi} e^{jm\phi_i}\, d\phi_i = 0 \quad ; \text{ for all integer } m \neq 0.$$

Thus, we conclude that

$$E(I(\omega_i,L)I^*(\omega_i,L)) = B^2P^3\, e^{-2\alpha L} \sum_a \sum_b \sum_c \frac{\delta(i-(a+b-c))}{\Delta k_i^2 + 4\alpha^2}$$

$$\cdot \left[1 + e^{-4\alpha L} - 2e^{-2\alpha L}\cos\Delta k_i L \right].$$

Appendix B

Derivation of $M_N(i)$

In this appendix we calculate the number of permutations such that i= a+b-c given that $a,b,c \neq i$; $M_N(i)$. We will start by finding the number of permutations such that i = a+b-c for $1 \leq a,b,c,i \leq N$. We begin by defining

$$f(k)= \begin{cases} 1 \; ; \; 1 \leq k \leq N \\ 0 \; ; \; \text{otherwise} \end{cases}.$$

F(k) is analogous to a probability density. Going further with the analogy, a, b, and c can be considered to be iid random variables each with "probability density" f(k). Thus, $f_i(k)$ will be the number of permutations such that i= a+b-c, $1 \leq a,b,c,i \leq N$.

Since a,b, and c are independent, identically distributed random variables with density f(k) we know that

$$f_i(k)= f(k)*f(k)*f(-k).$$

After performing this three-fold convolution we find

$$f_N(i)= \begin{cases} 1/2(N^2+N) & ; \; i=1 \\ \sum_{j=N+2}^{N+i} [(2N+1)-j] + \sum_{j=i+1}^{N+1} [j-1] & ; \; 2 \leq i \leq N \end{cases}.$$

Thus, $f_N(i)$ gives the number of permutations such that i= a + b - c given that a, b, and c are between 1 and N inclusive. However, we want to find the number of permutations given the additional constraint that a,b and c do not equal i. We can determine this quantity by first finding the number of permutations that include i and then subtract those from the total number of permutations, $f_N(i)$. There are two types of permutations that include i. They are:

A) i = i + a - a

B) i = a + b - i.

We can determine by observation that there are 2(N-1)+1 permutations such that i=i+a-a (2(N-1) permutations for a≠i and 1 permutation for a=i). For i=a+b-i, the number of permutations of such that a+b=2i. For $i \leq N/2$, this number is (i-1). For $i \geq N/2$, this number is (N-i). Therefore subtracting these numbers from $f_N(i)$ we conclude the number of permutations such that i=a+b-c given that a,b,c are between 1 and N and do not equal i is

$$M_N(i) = \begin{cases} \sum_{j=N+2}^{N+i} [2N+1-j] + \sum_{j=i+1}^{N+1} [j-1] - [2(N+i)-3] \; ; \; 2 \leq i \leq N/2 \\ \sum_{j=N+2}^{N+i} [2N+1-j] + \sum_{j=i+1}^{N+1} [j-1] - [4N-2i-1] \; ; \; N/2 < i \leq N \end{cases}$$

Finally, putting $M_N(i)$ in closed form we conclude

$$M_N(i)=\begin{cases} N(N+2i-2) - (1/2)[(N+i)(N+i+1)+i(i+1)] + 3 & ; 2\leq i\leq (N/2) \\ N(N+2i-4) - (1/2)[(N+i)(N+i+1)+i(i+1)] + (4i+1) & ; N/2<i\leq N \end{cases}$$

Appendix C

Derivation of Receiver Structure and Performance for the Synchronous Case

In this appendix we will derive the a posteriori densities for the received signal vector, the optimal detector structure, and it's corresponding performance for the synchronized pulse case. We will divide this analysis into two sections; first the derivation of the a posteriori densities and then the optimal receiver and it's performance.

Derivation of the A Posteriori Densities

In this section we will sample the received signal and determine the a posteriori densities for that representation. From Chap. III we know the received signals under H_1 and H_o are

$$\bar{r}(t|H_1) = \bar{s}(t) + \bar{I}(\omega_i, L) + \bar{n}(t)$$

$$r(t|H_o) = \bar{I}(\omega_i, L) + \bar{n}(t)$$

$$\text{where } s(t) = Ee^{-\alpha L} \begin{bmatrix} \cos\phi_i \\ \sin\phi_i \end{bmatrix}$$

and

$$\bar{I}(\omega_i, L) = \begin{bmatrix} \mathrm{Re}[I(\omega_i, L)] \\ \mathrm{Im}[I(\omega_i, L)] \end{bmatrix}.$$

$\bar{I}(\omega_i,L)$ is a zero mean Gaussian random variable with correlation matrix

$$\bar{R}_I(\omega_i,L)= \sigma_I^2\ \bar{I}$$

and $\bar{n}(t)$ is a zero mean Gaussian random process with correlation matrix

$$R_n(\tau)= (N_o/2)\delta(\tau)\ \bar{I}.$$

Since the real and imaginary parts of $\bar{r}(t)$ are independent we know that the joint density for the real and imaginary parts of the received signal is just the product of the marginal densities. Thus, we will now find the marginal densities for the sampled representation of the received signal. First, for the received signal under H_o we define

$$f(\bar{r}_r|H_o,\ I_r)= (2\pi\sigma_n^2)^{-k/2}\ \exp\left[\ -(1/2\sigma_n^2)\sum_{j=1}^{k}(r_r(t_j) - I_r)^2\ \right]$$

where $\bar{r}_r = (\ r_r(t_1)\ r_r(t_2).....r_r(t_k)\ )$; sampled Re(r(t))

and $I_r = Re[I(\omega_i,L)]$.

Averaging over I_r to decondition we find

$$f(\bar{r}_r|H_o)= \frac{[\sigma_n^2/(k\sigma_I^2 + \sigma_n^2)]^{1/2}}{(2\pi\sigma_n^2)^{k/2}}$$

$$\cdot\exp\left[-(1/2\sigma_n^2)\sum_{j=1}^{k} r^2(t_j)\right]\exp\left[\frac{\sigma_I^2/(k\sigma_I^2+\sigma_n^2)}{2\sigma_n^2}\left[\sum_{j=1}^{k} r_r(t_j)\right]^2\right]$$

which is also the same expression for $f(\bar{r}_I|H_o)$ (just change the r subscript into I) where $\bar{r}_I$ is the sampled version of the imaginary part of r(t).

Now, for the a posteriori density under H_1

$$f(\bar{r}_r|H_1,\ I_r)= (2\pi\sigma_n^2)^{-k/2}\ \exp\left[\ -(1/2\sigma_n^2)\sum (r_r(t_j) - I_r - s_r)^2\ \right].$$

where $s_r= Ee^{-\sigma L}\cos\phi_i$ and $s_I= Ee^{-\alpha L}\sin\phi_i$.

Deconditioning as before we find

$$f(\bar{r}_r|H_1) = \frac{[\sigma_n^2/(k\sigma_I^2+\sigma_n^2)]^{1/2}}{(2\pi\sigma_n^2)^{k/2}} \exp\left[-(1/2\sigma_n^2)\sum_{j=1}^{k} r_r^2(t_j)\right]$$

$$\cdot\exp\left[-(1/2\sigma_n^2)\sum_{j=1}^{k} s_r^2 - 2r_r(t_j)s_r\right]$$

$$\cdot\exp\left[\frac{\sigma_I^2/(k\sigma_I^2+\sigma_n^2)}{2\sigma_n^2}\left[k^2s_r^2 - 2ks_r\sum_{j=1}^{k} r_r(t_j)\right]\right]$$

$$\cdot\exp\left[\frac{\sigma_I^2/(k\sigma_I^2+\sigma_n^2)}{2\sigma_n^2}\left[\sum_{j=1}^{k} r_r(t_j)\right]^2\right]$$

By exchanging I for r in the subscripts, a similar expression is obtained for $f(\bar{r}_I|H_1)$. This expressions can now be used to determine the optimal receiver.

Derivation of Optimal Receiver

Our optimal receiver is of the form

$$\frac{f(\bar{r}|H_1)}{f(\bar{r}|H_o)} \begin{matrix} \hat{s}_1 \\ \geq \\ \leq \\ \hat{s}_o \end{matrix} 1$$

where $\bar{r} = (\bar{r}_r, \bar{r}_I)$

Using the marginal densities we transform this to

$$\frac{f(\bar{r}_r|H_1)\ f(\bar{r}_I|H_1)}{f(\bar{r}_r|H_o)\ f(\bar{r}_I|H_o)} \begin{array}{c} \hat{s}_1 \\ \geq \\ \leq \\ \hat{s}_o \end{array} 1.$$

Plugging in our expressions for the marginal densities and taking the natural log of both sides of the equation we obtain

$$\sum_{j=1}^{k} [r_r(t_j)s_r + r_I(t_j)s_I] \begin{array}{c} \hat{s}_1 \\ \geq \\ \leq \\ \hat{s}_o \end{array} (k/2)(s_r^2 + s_I^2).$$

Plugging in the expressions for s_r and s_I we obtain

$$\sum_{j=1}^{k} [r_r(t_j)\cos\phi_i + r_I(t_j)\sin\phi_i\ ] \begin{array}{c} \hat{s}_1 \\ \geq \\ \leq \\ \hat{s}_o \end{array} (k/2)E\ e^{-\alpha L}.$$

In continuous form this becomes

$$\int_0^T [\ r_r(t)\cos\phi_i + r_I(t)\sin\phi_i\ ]dt \begin{array}{c} \hat{s}_1 \\ \geq \\ \leq \\ \hat{s}_o \end{array} (TE/2)e^{-\alpha L}$$

where T is the pulse duration.

Performance Analysis

Defining $\gamma = \int_0^T [\, r_r(t)\cos\phi_i + r_I(t)\sin\phi_i \,]dt$ we see

$$\gamma = \int_0^T [\cos\phi_i(s_r + I_r + n_r(t)) + \sin\phi_i(s_I + I_I + n_I(t))\,]dt \;;\; \text{given } H_1$$

and

$$\gamma = \int_0^T [\cos\phi_i(\, I_r + n_r(t)) + \sin\phi_i(\, I_I + n_I(t))\,]dt \;;\; \text{given } H_o.$$

From these we find

$$f(\gamma|H_1) = N(\, TEe^{-\alpha L},\ (T^2\sigma_I^2 + T\sigma_n^2)\,)$$

and

$$f(\gamma|H_o) = N(\, 0,\ (T^2\sigma_I^2 + T\sigma_n^2)\,).$$

Using these densities, we conclude the probability of error, $Pr(\epsilon)$, for the synchronized case is

$$Pr(\epsilon) = Q\left[\, (1/2)Ee^{-\alpha L}\ (\, \sigma_I^2 + (N_o/2T)\,)^{-1/2}\,\right].$$

Appendix D

Derivation of Raman Fade Density

Here we derive the density for the signal corrupted by Raman fading. The signal can be described as a function of the random variable X by

$$E(\omega_N,L)= E(0)e^{-\alpha L} \exp[\ -(L_{eff}P(0)/A_{eff})X\ ]$$

where X is Gaussian with

$$E(X)= P\sum_i \gamma_i \qquad \text{and} \qquad \sigma_x^2 = (P-P^2)\sum_i \gamma_i^2\ .$$

Using the method of events, we will find the cumulative distribution function of $E(\omega_N,L)$ and, by differentiating, it's probability density function. The cumulative distribution function is defined as

$$F_{\leq E}(\ E(\omega_N,L)\ )= Pr(\ E(\omega_N,L)\leq E\ ).$$

Plugging in our expression we find

$$F_{\leq E}(\ E(\omega_N,L)\ )= Pr(\ E(0)e^{-\alpha L} \exp(\ -(L_{eff}P(0)/A_{eff})X\ ) \leq E\ ).$$

Working with the argument of Pr($\cdot$) the inequality reduces to

$$X \geq -(A_{eff}/L_{eff}P(0))(\ \ln(E) + \alpha L - \ln(E(0))\ ).$$

Defining $\Sigma = -(A_{eff}/L_{eff}P(0))\ (\ln(E)+ \alpha L -\ln(E(0))$

we determine that

$$F_{\leq E} = \left(1/\sigma_x(2\pi)^{1/2} \right) \int_{\Sigma}^{\infty} \exp\left[-(X-E(X))^2/2\sigma_x^2 \right] dX.$$

Differentiating this integral it is easy to show that

$$f(E)= \frac{A_{eff}/EP(0)L_{eff}}{\sigma_x(2\pi)^{1/2}} \exp\left[\frac{-(\ln E +\alpha L -\ln E(0) +(E(X)L_{eff}P(0)/A_{eff}))^2}{2(\sigma_x L_{eff}P(0)/A_{eff})^2} \right]$$

which is a log-normal density. The mean and variance for this distribution are

$$E(E)= E(0)e^{-\alpha L}\exp\left[-(E(X)L_{eff}P(0)/A_{eff}) + (\sigma_x L_{eff}P(0)/A_{eff})^2 \right]$$

$$\sigma_E^2 = E^2(0)e^{-2\alpha L} \exp\left[(\sigma_x L_{eff}P(0)/A_{eff})^2 - (E(X)L_{eff}P(0)/A_{eff}) \right]$$

$$\cdot\left(\exp\left[(\sigma_x L_{eff}P(0)/A_{eff})^2 \right] - 1 \right).$$

References

[**Abernathy 86**] Abernathy, J.D., The Effects of Nonlinearities on Frequency Multiplexed Communication Systems Utilizing Single Mode Optical Fiber, Ph.D. Dissertation Proposal M.I.T., May 1986

[**Arthurs**] Arthurs, E., Dym, H., On the Optimum Detection of Digital Signals in the Presence of White Gaussian Noise, IRE Transactions on Communication Systems, Dec. 1963, pp. 336

[**Chraplyvy 83**] Chraplyvy, A.R., Optical Power Limits in Multi-Channel Wavelength-Division-Multiplexed Systems Due to Stimulated Raman Scattering, Electronics Letters 1983, Vol. 20

[**Cotter**] Cotter, D., Stimulated Brillouin Scattering in Monomode Optical Fiber, J. of Communications 4 (1983), pp. 10-19

[**Halme 69**] Halme, S.J., Efficient Optical Communication in a Turbulent Atmosphere, Ph.D. Dissertation M.I.T., Feb. 1970

[**Henry 83**] Chraplyvy, A.R., Henry, P.S., Performance Degradation Due to Stimulated Raman Scattering in Wavelength-Division-Multiplexed Optical Fiber Systems, Electronics Letters, 1983, 19, pp. 641-643

[**Hill 78**] Hill, D.O., Johnson, D.C., Kawasaki, B.S., MacDonald, R.I., CW Three-Wave Mixing in Single Mode Optical Fibers, J. of Applied Physics, Oct. 1978, pp. 5098-5106

[**Ippen 85**] Ippen, E.P., Nonlinear Optics Course Notes, M.I.T., 1985

[**Pocholle 85**] Pocholle, J.P., Raffy, J., Papuchon, M.,Desurvire, E., Raman and Four Photon Mixing Amplification in Single Mode Optical Fibers, Optical Engineering, July/August 1985, Vol. 24 No. 4, pp. 600-608

[Shen 84] Shen, Y.R., The Principles of Nonlinear Optics, John Wiley & Sons, 1984

[Shibata 86] Shibata, N., Braun, R.P., Waarts, R.G., Crosstalk Due to Three Wave Mixing in a Coherent Single-Mode Transmission Line, Electronics Letters, 1986, 22, pp. 675

[Smith 72] Smith, R.G., Optical Power Handling Capacity of Low Loss Optical Fibers as Determined by Stimulated Raman Scattering and Brillouin Scattering, Applied Optics, Nov. 1972, Vol. 11, No. 11, pp. 24989-2494

[Stolen 75] Stolen, Rogers H., Phase-Matched Stimulated Four Photon Mixing in Silica Fiber Waveguides, IEEE J. of Quantum Electronics, Vol. QE-11, No. 3, March 1975

[Stolen 79] Ibid, Nonlinear Properties of Optical Fibers, Optical Fiber Telecommunications, Pub. 1979, Bell Telephone Laboratories

[Stolen 80] Ibid, Nonlinearity in Fiber Transmission, Proceedings of the IEEE, Vol. 68, No. 10, Oct. 1980

[Stolen 82] Ibid, Parametric Amplification and Frequency Conversion in Optical Fibers, IEEE J. of Quantum Electronics, Vol. QE-18, No. 7, July 1982

[Tomita 83] Tomita, A., Crosstalk Caused by Stimulated Raman Scattering in Single-Mode Wavelenth Division Multiplexed Systems, Optics Letters, Vol. 8, No. 7, July 1983

[Van Trees] Van Trees, H.L., Detection, Estimation, and Modulation Theory Part I, Wiley, 1968

[Waarts 86] Waarts, R.G., Braun, R.P. System Limitations Due to Four-Wave Mixing in Single Mode Optical Fibers, Electronics Letters, 1986, 22, pp. 87